

# Evaluating Policy Effects through Network Dynamics and Sampling

Eugene T.Y. Ang\*, Yong Sheng Soh\*<sup>†</sup>

## Abstract

In the process of enacting or introducing a new policy, policymakers frequently consider the population's responses. These considerations are critical for effective governance. There are numerous methods to gauge the ground sentiment from a subset of the population; examples include surveys or listening to various feedback channels. Many conventional approaches implicitly assume that opinions are static; however, in reality, the population will discuss and debate these new policies among themselves, and reform new opinions in the process. In this paper, we pose the following questions: Can we quantify the effect of these social dynamics on the broader opinion towards a new policy? Given some information about the relationship network that underlies the population, how does overall opinion change post-discussion? We investigate three different settings in which the policy is revealed: respondents who do not know each other, groups of respondents who all know each other, and respondents chosen randomly. By controlling who the policy is revealed to, we control the degree of discussion among the population. We quantify how these factors affect the changes in policy beliefs via the Wasserstein distance between the empirically observed data post-discussion and its distribution pre-discussion. We also provide several numerical analyses based on generated network and real-life network datasets. Our work aims to address the challenges associated with network topology and social interactions, and provide policymakers with a quantitative lens to assess policy effectiveness in the face of resource constraints and network complexities.

arXiv:2501.08150v1 [cs.SI] 14 Jan 2025

---

\*Institute of Operations Research and Analytics (IORA), National University of Singapore (NUS)

<sup>†</sup>Department of Mathematics, National University of Singapore (NUS)

# 1 Introduction

Rigorous policy design, analysis and evaluation are essential to good governance (OECD, 2020). Apart from evaluating whether a policy has produced the desired results or pinpointing the elements that have either facilitated or impeded the policy efficacy, it is also imperative to discern how the population or target audience reacts and adapts to the policy. The level of public reception gives the policymakers an indication of public confidence in the policy (Grelle & Hofmann, 2024). Furthermore, it provides telltale signs of plausible shortcomings, drawbacks and resistance. By identifying areas where the policy may fall short, policymakers can proactively address these challenges and make necessary adjustments to enhance its effectiveness and mitigate adverse impacts on the population.

The gold standard for assessing the efficacy of policies is to employ randomized controlled trials (RCTs) (Hariton & Locascio, 2018). Apart from the practical or ethical concerns (Goldstein et al., 2018), there are methodological challenges. It is often difficult to isolate the respondents in the population and the confounding factors that affect one’s behavior and actions. For instance, respondents generally interact among themselves and influence each other in the process. The result is that the collective may arrive at a consensus that is quite different before the interaction (Larsen, 1990; Abrams & Levine, 2012; Sherif, 1937), and such behavior may affect the overall policy effectiveness (Burstein, 2003). As an example, the government of a certain country might wish to implement a vaccination campaign to control the spread of a contagious disease such as COVID-19. Interactions within their social circles can influence individuals’ decisions to get vaccinated. To make the situation more complex, the presence of vaccine skeptics may (adversely) affect the vaccine take-up rate in the nation (Allen et al., 2024). Hence, policymakers need to discern and evaluate the initial policy beliefs within the population before influential individuals shape public opinion prematurely.

To evaluate a policy effectively, not only do policymakers need an accurate assessment of the initial beliefs and responses towards the policy, policymakers also need some understanding as to how these opinions might evolve and reform as respondents discuss among themselves. More often than not, these interactions and fine-grained changes in beliefs are not reflected in empirical data due to infrequent data collection processes and policymakers need to resort to statistical inference to estimate such deviations. Furthermore, individual response to policies is sometimes not binary due to one’s ambivalence (Persson, 2021), hence it is important to design an appropriate policy evaluation study to accommodate a range of responses. Certain evaluation exercises such as polls and referendums with categorical options might not be able to capture the nuances in public opinion. For example, the UK had a referendum on the intricate Brexit issue in 2016, where the ballot had two options, namely “Leave” and “Remain”. Although the referendum produces an outcome with the majority votes, these blunt options can be difficult to interpret and voters cannot express their opinions constructively (Van Crombrugge, 2021; Wagenaar, 2019).

Besides designing sophisticated studies, policymakers often face resource and feasibility con-

straints. Certain information may not be available to these policymakers such as individuals' covariates like income and age; and network connections due to legal constraints, for instance, the Personal Data Protection Act (PDPA) in Singapore and the General Data Protection Regulation (GDPR) in European Union and the European Economic Area. Thus, the policymakers might only have access to limited population data to ascertain the public opinion of the policy. Moreover, conducting periodic population-wide consensus surveys is time-consuming and resource-intensive. Realistically, policymakers are only able to survey a small group of people in a single time instance to infer the population's opinion.

## 1.1 Our contributions

The main objective of this work is to understand the impact of social dynamics and interaction on the population's opinion towards policies. Concretely, we build a model that describes a population's response towards a new policy. As time passes, the population is given the opportunity to discuss the newly announced policy, and may reform their personal assessments and opinions. Our central question is to quantify the size of these changes based on the characteristics of the social networks that underlie the population.

The policymaker is ultimately aware that the population will discuss these policies among themselves, and may be interested in understanding the population's general response at different stages: one closer to the initial stages where opinions are raw, relatively uninformed, and possibly quite diverse, or in the later post-discussion stages where the policy has been extensively debated and a broader consensus may be reached. To obtain the opinion polls at different stages, we assume that policymakers can select the subset of respondents they wish to reveal the policy to. By doing so, policymakers have control over the amount of interaction between the respondents. There are several ways policymakers can do so. For example, the policymakers can select groups of respondents who do not know one another and are unlikely to interact within themselves, allowing policymakers to estimate initial policy responses free from the effects of interactions (Ang et al., 2025; Karwa & Airoidi, 2018; Fatemi & Zheleva, 2023). However, it is impractical to attempt to recruit groups of respondents who do not know each other because this assumes some knowledge about existing relationships among the population (e.g., through social media platforms). Policymakers can consider alternative strategies, such as randomly selecting a large group of respondents without regard for the underlying relationships, in the hope that the gains from estimating from a larger sample size are not severely corrupted by the effects of discussion among the respondents. In estimating the initial policy responses, policymakers face a tradeoff between the size of the subset of respondents and the potential network interaction effect.

In our work, we characterize the network interaction and the sample size effects. We provide quantitative bounds on how the population opinion changes across different sampling techniques, network topologies, and interaction contexts. We conduct numerical experiments using generated and real-life networks to illustrate the tradeoff between the sample size and the in-

teraction effect on various network topologies. We describe how sparsity in the relationship network – by extension a measure of the number of relationships relative to the population size – plays a critical role in the estimation accuracy. Coupled with various sampling strategies, they shape the influence of network interactions within the respondents and the sample size, thus highlighting the interplay of both effects on estimating the initial policy responses. We illustrate specific instances where either effect dominates the other.

## 1.2 Paper layout

In the following section, we discuss past work on modeling opinion dynamics and policy evaluation methodologies that are used to estimate policy effects. We formally formulate the problem in Section 3 and present the main results in Section 4. Subsequently, in Section 5, we investigate how different graphical networks and interaction contexts affect the estimation. Lastly, in Section 6, we conduct several numerical experiments based on various generative and real-life networks, different interaction contexts, and dissimilar initial belief distributions. We then illustrate the insights from these numerical simulations.

## 2 Related Work

In this section, we discuss the current literature on various opinion dynamics models and present several existing policy evaluation methodologies that leverage observational data to estimate the policy effects in networked settings.

### 2.1 Effect of Opinion Dynamics

The implementation of a new policy prompts discussions among people and these interactions influence their beliefs and behaviors regarding the policy. As public opinion plays an important role in determining the effectiveness of the policy (Jones & Jenkins-Smith, 2009), it is important to understand and explore how consensus and polarization develop over time. One can adopt a data-driven approach by analyzing large-scale social data on communication platforms (González-Bailón, 2013). However, these data may not be entirely available due to legal or confidentiality issues. Hence, the sparsity of these data and the complexity in the data collection process call for realistic modeling of opinion formation and interaction (Peralta et al., 2022; Sobkowicz, 2009; Castellano et al., 2009). There are several notable opinion dynamics models such as the voter model (Holley & Liggett, 1975; Redner, 2019), DeGroot model (DeGroot, 1974) and bounded confidence model (Lorenz, 2007; Hegselmann, Krause, et al., 2002; Deffuant et al., 2000). These models assign an opinion state variable to every individual, and these variables change over time based on the system’s stipulated mechanism. The resulting systemic state usually depends on the underlying graphical structure (Castellano et al., 2009; Golub & Jackson, 2010; Xia et al., 2011). These models help to explain the formation of collective opinions, the shift in beliefs due to peer and social influence and the emergence of social consensus or division. Although most opinion dynamics literature focuses on the resulting state of the system, our work incorporates these mechanisms into a policy evaluation setting. Through modeling the interactions and opinion dynamics, the policymakers can then gauge the initial

distribution of the population belief and quantify the evolution of the policy beliefs. This aids them in inferring the policy impact through statistical inference.

## 2.2 Challenges in Policy Evaluation Methods

It is difficult to assess policy effectiveness as behaviors and beliefs are largely influenced by the individual’s social connection. This influence potentially confounds the evaluation of policy effects and complicates the assessment of its overall effectiveness. Addressing the role of network influence in policy evaluation requires stakeholders to adopt rigorous experimental methods executed with nuanced sophistication (Athey & Imbens, 2017). Some studies use randomization inference to estimate the treatment effect in the presence of network interference (Bowers et al., 2013; Aronow, 2012), while others construct statistical estimators to estimate the policy effects (Forastiere et al., 2021; Leung, 2020; Tchetgen & VanderWeele, 2012). There is also a stream of work that uses the linear-in-means model (Aronow & Samii, 2017; Cai et al., 2015), which estimates the average treatment effect based on the aggregated individuals’ covariates (Kline & Tamer, 2014; Manski, 1993).

We note that most policy studies make use of fine-grained information such as individuals’ beliefs and demographic covariates, to aid with the estimation of the policy effects. However, due to certain constraints and restrictions, policymakers do not necessarily have complete access to such information. The incomplete data, on top of the possible interaction between the selected policy-exposed respondents, inhibits the performance of these models and statistical estimators, thus creating a discrepancy in the estimates. Policymakers could account for this discrepancy by computing the distance between the initial and empirically observed belief distributions. Some popular distance metrics include Wasserstein and total variation or divergences such as Kullback-Leibler (KL) and Jensen-Shannon (Cai & Lim, 2022). In our paper, we consider the Wasserstein metric as it is amenable for analysis, making it appropriate for statistical inference. The Wasserstein distance is a special instance of the optimal transport problem, where it can be viewed as the smallest effort to shift the mass of one distribution to recover the other (Villani et al., 2009). Notably, it has various applications in machine learning (Frogner et al., 2015; Leo et al., 2023), economics (Gini, 1914) and finance (Rachev & Rüschendorf, 1998). By quantifying the distance between the initial and empirically observed belief distributions using the Wasserstein metric, we distil the effects of interaction and the sample size, which we then illustrate their tradeoff analytically and numerically.

## 3 Problem Formulation

Suppose a policymaker wishes to implement a specific policy on the population denoted by  $P$ . We model the internal (private) response of each respondent in  $P$  as a scalar random variable  $X_i$  that is drawn i.i.d. from a *unknown* distribution  $\mathcal{F}^*$

$$X_i \sim \mathcal{F}^*, \quad X_i \in \mathbb{R}.$$

We denote the mean and standard deviation of  $\mathcal{F}^*$  by  $\mu$  and  $\sigma$  respectively.<sup>1</sup>

Policymakers are ultimately interested in understanding the population’s receptiveness towards a policy. We model this process as trying to estimate the unknown distribution  $\mathcal{F}^*$ . The policymaker does so by drawing some observations from  $\mathcal{F}^*$ ; for instance, by performing a survey. Unfortunately, this process is complicated by the fact that the people within the population communicate among themselves, and in the process influence each other’s opinion of the policy. While it is in principle possible for the policymaker to survey every respondent and track their responses periodically so as to understand how their opinions form and alter, this approach is simply too expensive to be practical. Instead – and realistically speaking – policymakers are only able to conduct a survey of the population’s opinion in a single time instance. Moreover, surveys are usually difficult to design and expensive to set up. By the time a survey is conducted, a substantial amount of time would have lapsed for the population to interact and reform opinions.

We model the relationships within the population as a graph  $G(P, E)$ , where the population  $P$  forms the set of vertices, and where the edges  $E$  represent the relationship between pairs of respondents. We distinguish between two scenarios: (i) where the relationships are mutual, in which case we model these relationships as an undirected graph  $G$ , and (ii) where relationships may be directed (e.g., a regular respondent who views social media posts by an influential person), in which case we model these relationships as a directed graph  $G^d$ . The degree of the sampled respondent  $i$  is the number of connections  $i$  has, which is denoted by  $d_i$ . Similarly, the outdegree of  $i$  is the number of directed connections from  $i$ , which is denoted by  $d_i^o$ .

In this paper, we assume that policymakers can decide who they wish to reveal the policy to. We let  $S \subseteq P$  denote the subset of the population that the policymakers reveal the policy. There is an advantage in restricting access. For instance, if we are able to only reveal the policy to a subset of the population who do not know each other, we minimize the possibility that these people interact and affect each other’s opinions. For simplicity, we also take  $S$  as the subset of the population the policymakers eventually survey from in our subsequent discussions. We let  $\hat{\mathcal{F}}_{|S|}$  denote the empirical distribution of these responses.

Next, we model how people influence each other’s opinions. We describe the dynamics via a stochastic matrix. Suppose that the policymakers reveal the policy to  $n$  respondents. Given a stochastic  $n \times n$  adjacency matrix, where the entries  $a_{ij}$  capture the normalized tendency for respondent  $i$  to listen to respondent  $j$  after they interact (DeGroot, 1974). After interacting, respondent  $i$  updates and forms the opinion  $\sum_j a_{ij} X_j$ . In particular,  $a_{ij}$  is positive if vertices  $i$  and  $j$  are adjacent, i.e.  $i \sim j$ , and is zero otherwise, where  $\sum_j a_{ij} = 1$  for all  $i \in \{1, 2, \dots, n\}$ . This formulation allows a respondent  $i$  to forsake his/her own belief if  $a_{ii} = 0$ . We say that the sampled respondents follow the *average interaction rule* if they update their own beliefs by taking the average value of the beliefs of every respondent in the same clique, including his/her

---

<sup>1</sup>As a note, several opinion dynamics models such as the Deffuant-Weisbuch (DW) and the Hegselmann-Krause (HK) models have a bounded support interval of  $[0, 1]$  – here, we do not make such assumptions.

own, i.e.,  $a_{ik} = \frac{1}{|N_i|+1}$ , for  $k \in \{i\} \cup N_i$ , where  $N_i$  is the set of neighbors of respondent  $i$ , or 0 otherwise. The average interaction rule we adopt is a simple mechanism to capture the effect of interactions. There are settings where individuals may, for instance, place more emphasis on their personal opinions, or may listen to certain people more than others. In Section 5, we discuss extensions where the opinions are formed by weighing the opinions of neighbors differently; i.e., through the *weighted average interaction rule*.

### 3.1 Sampling Strategies

In this section, we describe how a subset of respondents is selected. We describe different sampling strategies and discuss their implications in the estimation process.

**Independent Set Sampling** (Ang et al., 2025; Karwa & Airoidi, 2018; Fatemi & Zheleva, 2023). In this setting, the policy is revealed to a subset of  $n$  respondents that are carefully chosen such that these respondents do not know one another. The group of respondents form an independent set in the relationship graph – every pair of respondents does not communicate with one another. In particular, their beliefs remain unchanged between the revelation of the policy and the subsequent conduct of the survey. Policymakers are then able to estimate the initial belief distribution provided they have surveyed sufficiently many respondents.

Suppose the samples being drawn i.i.d. from the same underlying  $\mathcal{F}^*$ , then the Strong Law of Large Numbers (SLLN) tells us that

$$\hat{F}_n(t) \xrightarrow{a.s.} F(t) \text{ as } n \rightarrow \infty,$$

for every value of  $t$ , where  $\hat{F}_n$  is the empirical cumulative distribution function (ecdf) of  $\hat{\mathcal{F}}_n$  and  $F$  is the cumulative distribution function (cdf) of  $\mathcal{F}^*$ . In other words, one is able to accurately estimate – and without any *bias* – the population’s sentiment provided the sample size is sufficiently large.

In general, and as in all estimation problems, having as many samples as our budget allows is preferred. There are two drawbacks to the independent set sampling strategy. First, and most crucially, it assumes that policymakers have knowledge about the graph  $G$  – that is, they know the relationships among its population. This is an extremely strong assumption and can be unrealistic in certain policy contexts. The second downside is that requiring the set of respondents to form an independent set (in the relationship graph  $G$ ) places a hard limit on the number of samples one can draw, and this depends on the graphical structure. If the average person knows a substantial fraction of the population; i.e., the average degree of the graph  $G$  is high, then we are only able to select a small number of respondents while ensuring that none of them know each other. For instance, the following result by Kwok (West, 1996) describes an upper bound on the size of the independent set based on the maximum degree of the network.

**Theorem 1.** *Let  $G(V, E)$  be a graph and let  $\Delta$  be the maximum degree in  $G$ . Then, the size of*

the largest independent set of  $G$ ,  $\alpha(G)$ , has the following upper bound,

$$\alpha(G) \leq |V| - \frac{|E|}{\Delta}$$

**Random Sampling.** In the independent set sampling strategy, we assume perfect knowledge about the underlying relationship network  $G$  and we sample respondents based on knowledge of  $G$ . The random sampling strategy does the exact opposite – we simply sample from a large pool without regard for the underlying relationship between respondents. In doing so, we are potentially able to sample from a larger pool of respondents. The downside is that there may be a fraction of respondents who know each other – that is, they share edges in  $G$ . The policymakers have no control over this process. These respondents may communicate about the policies among themselves before we are able to survey their response, and in the process, update their internal response to the policies.

**Cluster/Clique Sampling** (Ugander et al., 2013; Ugander & Yin, 2023; Eckles et al., 2017). In the clique sampling strategy, policymakers draw observations from a subset of respondents that belong to disjoint cliques. Concretely, we assume that the policymakers sample  $p$  cliques each of size  $r$ ,  $C_1, C_2, \dots, C_p$ , where  $n = pr$ . The resulting subgraph  $\tilde{G}$  denotes the relationship within these sampled respondents, where

$$\begin{cases} e_{ij} \in \tilde{E} & \text{if } i, j \in C_k \text{ for } k \in \{1, 2, \dots, p\} \\ e_{ij} \notin \tilde{E} & \text{if } i \in C_k, j \in C_l \text{ for } k \neq l \end{cases}$$

Respondents within the same clique interact with each other and influence each other’s opinions. Respondents from different cliques, on the other hand, do not interact. The cluster/clique sampling strategy is a stylized model whose purpose is to help us understand how certain attributes about communities (such as the size of the communities  $r$  as well as the number of different communities  $p$ ) affect our estimation of  $\mathcal{F}^*$ .

After illustrating the sampling strategies that the policymakers use, we explain how policymakers can account for the discrepancies between the observed belief distribution  $\hat{\mathcal{F}}_n$  and the initial belief distribution  $\mathcal{F}^*$  in the next section.

## 4 Quantifying the distance between $\hat{\mathcal{F}}_n$ and $\mathcal{F}^*$

The main source of information policymakers have to infer the response of the entire population is the surveyed responses from the sampled population. Based on these responses, the policymakers form an estimate of the underlying distribution of the population’s private (unknown) response, which in turn forms the basis of their evaluation of the policies. As such, it is of interest to understand how the estimated distribution differs from the true underlying distribution.

Specifically, policymakers collect surveyed responses  $\{X_i\}_{i=1}^n$ . Using these responses, the policymaker obtains an empirical distribution  $\hat{\mathcal{F}}_n$  using the empirical data, which then serves as



a comparison to the underlying unknown distribution  $\mathcal{F}^*$ . Both  $\hat{\mathcal{F}}_n$  and  $\mathcal{F}^*$  are probability distributions, so a natural way to compare these is to deploy a suitable distance measure over probability distributions.

## 4.1 Optimal Transport Distance

In this paper, we quantify the difference between probability distributions using the Wasserstein distance.

The Wasserstein distance is a special instance of the optimal transport (OT) problem, which seeks optimal transportation plans between probability distributions so as to minimize cost. Concretely, let  $\alpha \in \Delta_m$  and  $\beta \in \Delta_n$  be probability distributions over a metric space – here,  $\Delta_m = \{\alpha \in \mathbb{R}_+^m, \sum_{i=1}^m \alpha_i = 1\}$  denotes the probability simplex. Let  $C \in \mathbb{R}^{m \times n}$  be the matrix such that  $C_{i,j}$  models the transportation cost between points  $x_i \sim \alpha$  and  $y_j \sim \beta$ . The Wasserstein distance is defined as the solution of the following convex optimization instance

$$\pi_W = \underset{\pi}{\operatorname{arg\,min}} \langle C, \pi \rangle \quad \text{s.t.} \quad \pi \in \Pi(\alpha, \beta) \quad (1)$$

where  $\Pi(\alpha, \beta) = \{\pi \in \mathbb{R}_+^{m \times n} : \pi \mathbf{1}_n = \alpha, \pi^T \mathbf{1}_m = \beta\}$  denotes the set of couplings between probability distributions  $\alpha \in \Sigma_m, \beta \in \Sigma_n$  while  $\mathbf{1}_m \in \mathbb{R}^m$  denotes the vector of ones.

The OT problem (1) is an instance of a linear program (LP), and hence admits a global minimizer. The  $p$ -Wasserstein distance between probability measures  $\xi$  and  $\nu$  on  $\mathbb{R}^d$  is defined as follows,

$$W_p(\xi, \nu) = \left( \inf_{\pi \in \Pi(\xi, \nu)} \int d(x, y)^p d\pi(x, y) \right)^{1/p}$$

In the special case where the underlying metric space is the real line  $\mathbb{R}$ , and where cost between two points  $x$  and  $y$  is given by the absolute value  $|x - y|^p$ , the  $p$ -Wasserstein distance admits a simpler expression:

$$W_p(\xi, \nu) = \left( \int_0^1 |G_1^{-1}(q) - G_2^{-1}(q)|^p dq \right)^{1/p}$$

where  $\xi$  and  $\nu$  are probability measures on  $\mathbb{R}$ , and  $G_1^{-1}$  and  $G_2^{-1}$  are their respective inverse cumulative distribution functions (cdf). In particular, when  $p = 1$ , the 1-Wasserstein distance simplifies to the following:

$$W_1(\xi, \nu) = \int_{\mathbb{R}} |G_1(x) - G_2(x)| dx$$

where  $\xi$  and  $\nu$  are probability measures on  $\mathbb{R}$ , and  $G_1(x)$  and  $G_2(x)$  are their respective cdfs.

Suppose that the policymakers sample  $n$  respondents, where  $n < |P|$ . Given  $n$  i.i.d. samples  $X_1, X_2, \dots, X_n$  from the distribution  $\mathcal{F}^*$ , the empirical cumulative distribution function (ecdf) of their beliefs  $\hat{F}_n$ , is given as

$$\hat{F}_n(t) = \frac{1}{n} \sum_{i=1}^n \mathbf{1}(X_i \leq t)$$

The ecdf is a random measure. As such, to quantify how  $\hat{F}_n$  differs from  $F$ , we compute the expected 1-Wasserstein distance between  $\hat{F}_n$  and  $F$ . Next, we investigate how the various sampling strategies change the ecdf and its implications on the 1-Wasserstein distance.

## 4.2 Independent Set Sampling

As the independent set sampling strategy does not allow interactions between the sampled respondents, the observed belief distribution  $\hat{\mathcal{F}}_n$  is just the empirical version of the initial belief distribution  $\mathcal{F}^*$ . Then, the ecdf  $\hat{F}_n(t)$  is given as  $\frac{1}{n} \sum_{i=1}^n \mathbb{1}(X_i \leq t)$ . We note that, for a fixed  $t$ ,  $\mathbb{1}(X_i \leq t)$  is a Bernoulli random variable, where

$$\mathbb{1}(X_i \leq t) = \begin{cases} 1 & \text{w.p. } F(t) \\ 0 & \text{w.p. } 1 - F(t) \end{cases}$$

Then,  $\mathbb{E}[\hat{F}_n(t)] = F(t)$  and  $\text{Var}(\hat{F}_n(t)) = \frac{F(t)(1-F(t))}{n}$ .

**Proposition 1.** *The expected 1-Wasserstein distance between the ecdf  $\hat{F}_n$  and the cdf  $F$  has the following upper bound,*

$$\mathbb{E} \left[ W_1(\hat{F}_n, F) \right] \leq \frac{1}{\sqrt{n}} \int_{\mathbb{R}} \sqrt{F(t)(1-F(t))} dt$$

*Proof.*

$$\begin{aligned} \mathbb{E} \left[ W_1(\hat{F}_n, F) \right] &= \mathbb{E} \left[ \int_{\mathbb{R}} |\hat{F}_n(t) - F(t)| dt \right] \\ &\stackrel{(a)}{=} \int_{\mathbb{R}} \mathbb{E} \left[ |\hat{F}_n(t) - F(t)| \right] dt \\ &= \int_{\mathbb{R}} \mathbb{E} \left[ \sqrt{(\hat{F}_n(t) - F(t))^2} \right] dt \\ &\stackrel{(b)}{\leq} \int_{\mathbb{R}} \sqrt{\mathbb{E} \left[ (\hat{F}_n(t) - F(t))^2 \right]} dt \\ &= \int_{\mathbb{R}} \sqrt{\text{Var}(\hat{F}_n(t))} dt \\ &= \frac{1}{\sqrt{n}} \int_{\mathbb{R}} \sqrt{F(t)(1-F(t))} dt \end{aligned}$$

Here, (a) is by Fubini's Theorem and (b) is by Jensen's inequality.  $\square$

In particular, Proposition 1 tells us that the deviation between the initial and the empirically observed belief distributions vanishes at a rate of  $O(1/\sqrt{n})$ , where  $n$  is the number of sampled respondents. However, as we noted earlier, there is a hard limit to the value of  $n$  to which we can apply the result.

## 4.3 Clique Sampling

Next, we consider the clique sampling strategy where policymakers obtain a sample of  $n$  respondents by selecting  $p$  cliques of size  $r$  randomly. In this model, all respondents within the

same clique know each other and interact among themselves. On the other hand, pairs of respondents belonging to different cliques do not interact with each other. Following the average interaction rule, the updated beliefs of each respondent after interacting is a random variable whose distribution is equal to the sample mean distribution of  $r$  i.i.d. samples drawn from the distribution  $\mathcal{F}^*$ . In the following, we denote the sample mean distribution obtained by drawing  $r$  i.i.d. samples from  $\mathcal{F}^*$  by  $\mathcal{F}^r$ , and we denote the cdf of  $\mathcal{F}^r$  by  $F^r$ . Since all respondents within the same clique perform the same update, all of them share the same updated belief after interacting. Subsequently, the empirical distribution formed by the surveyed responses is equal to  $p$  i.i.d. draws random variables drawn from  $\mathcal{F}^r$ , and each observation is repeated with  $r$  copies. We denote the resulting ecdf by  $\hat{F}_p^r$ . Suppose we let  $\mu$  and  $\sigma$  denote the mean and the standard deviation of  $\mathcal{F}^*$ . Then, the mean and standard deviation of  $\mathcal{F}^r$  is  $\mu$  and  $\sigma/\sqrt{r}$  respectively. Since the 1-Wasserstein distance defines a metric, one has

$$\mathbb{E}[W_1(\hat{F}_p^r, F)] \leq \mathbb{E}[W_1(\hat{F}_p^r, F^r)] + \mathbb{E}[W_1(F^r, F)].$$

In the following, we bound the term  $\mathbb{E}[W_1(\hat{F}_p^r, F)]$  by analyzing the two error terms on the RHS. In particular, Proposition 1 allows us to bound  $\mathbb{E}[W_1(\hat{F}_p^r, F^r)]$  directly. As such, the next step is to understand how the sample mean distribution deviates from the original distribution, as a function of  $r$ . We are not aware if a simple expression that bounds  $\mathbb{E}[W_1(F^r, F)]$  for general distributions exists. However, explicit expressions for the 2-Wasserstein distances between normal distributions are well known. With the aid of the following theorem, we obtain a bound  $\mathbb{E}[W_1(F^r, F)]$  by approximating each of these distributions with a normal distribution with matching mean and variance.

**Theorem 2** (Equation 21 (Irpino & Verde, 2015)). *The decomposition of 2-Wasserstein distance between 2 distributions, where  $F_A$  and  $F_B$  are the corresponding cdfs and  $F_A^{-1}$  and  $F_B^{-1}$  the respective quantile functions, is given as,*

$$W_2^2(F_A, F_B) = (\mu_A - \mu_B)^2 + (\sigma_A - \sigma_B)^2 + 2\sigma_A\sigma_B(1 - \rho^{A,B})$$

where  $\mu_A$  and  $\mu_B$  are the respective means,  $\sigma_A$  and  $\sigma_B$  are the respective standard deviations, and  $\rho^{A,B}$  is the Pearson correlation of the points in the quantile-quantile plot of  $F_A$  and  $F_B$ .

Now, we derive the upper bound of the expected 1-Wasserstein distance between  $\hat{F}_p^r$  and  $F$ , with  $\tilde{F}$  and  $\tilde{F}^r$  be the respective cdfs of the normal distributions,  $N(\mu, \sigma^2)$  and  $N(\mu, \frac{\sigma^2}{r})$ .

**Proposition 2.** *Suppose the policymakers select  $n$  respondents such that there are  $p$  cliques of size  $r$ , where  $n = pr$ . The expected 1-Wasserstein distance between cdf of the initial belief distribution  $F$  and the ecdf of the observed belief distribution  $\hat{F}_p^r$  is given as*

$$\begin{aligned} \mathbb{E} \left[ W_1(F, \hat{F}_p^r) \right] &\leq \sigma \left( 1 - \frac{1}{\sqrt{r}} \right) + \frac{1}{\sqrt{p}} \int_{\mathbb{R}} \sqrt{F^r(t)(1 - F^r(t))} dt \\ &\quad + \sigma \sqrt{2(1 - \rho^{F, \tilde{F}})} + \sigma \sqrt{(2/r)(1 - \rho^{F^r, \tilde{F}^r})}, \end{aligned}$$

where  $\rho^{F, \tilde{F}}$  and  $\rho^{F^r, \tilde{F}^r}$  are the respective Pearson correlation of the points in the quantile-quantile plot of  $F$  and  $\tilde{F}$ , and  $F^r$  and  $\tilde{F}^r$ .

We explain the interpretation behind these bounds. First, the term  $\sigma(1 - \frac{1}{\sqrt{r}})$  captures the effect of cliques – namely, each respondent pays more attention to the opinions of others, and de-emphasizes his or her own opinions. When  $r = 1$ , the term is zero, and there is no deviation because each respondent does not communicate. When  $r$  is large, the error term is approximately  $\sigma$ , representing the other extreme where we get no information about the differences between opinions as we only observe a consensus among the respondents. The second term  $\frac{1}{\sqrt{p}} \int_{\mathbb{R}} \sqrt{F^r(t)(1 - F^r(t))} dt$  is analogous to Proposition 1 – in particular, more samples  $p$  leads to more effective estimation of  $F$ . For fixed  $n$ , the terms  $p$  and  $r$  represent an inherent tension – larger cliques that form consensus means that individuals lose their voice, and the effect is quantified in first row of the error terms.

We briefly comment on the error term  $\sigma\sqrt{2(1 - \rho^{F, \tilde{F}})} + \sigma\sqrt{(2/r)(1 - \rho^{F^r, \tilde{F}^r})}$  in the second row. These represent the error when approximating the distributions with a normal distribution. If the original distributions are suitably close to being normal, then the terms  $(1 - \rho^{F, \tilde{F}})$  and  $(1 - \rho^{F^r, \tilde{F}^r})$  are approximately zero, and we can ignore the contributions of these terms. We believe the presence of these terms is an artefact of our analysis – in particular, even if the original distribution  $\mathcal{F}^*$  is far from a normal distribution, we believe that the true error  $\mathbb{E} [W_1(F, \hat{F}_p^r)]$  should be dominated by the terms in the first row.

*Proof.* We note that there is an analytic solution of the 2-Wasserstein distance between two Gaussian distributions,  $\mathcal{G} = N(\mu_G, \sigma_G^2)$  and  $\mathcal{H} = N(\mu_H, \sigma_H^2)$ , which is given by

$$W_2^2(\mathcal{G}, \mathcal{H}) = (\mu_G - \mu_H)^2 + (\sigma_G - \sigma_H)^2 \quad (2)$$

Then, we have

$$\begin{aligned} \mathbb{E} [W_1(F, \hat{F}_p^r)] &\stackrel{(a)}{\leq} \mathbb{E} [W_1(F, F^r) + W_1(F^r, \hat{F}_p^r)] \\ &\stackrel{(b)}{\leq} W_1(F, \tilde{F}) + W_1(\tilde{F}, \tilde{F}^r) + W_1(\tilde{F}^r, \tilde{F}) + \mathbb{E} [W_1(F^r, \hat{F}_p^r)] \\ &\stackrel{(c)}{\leq} W_2(F, \tilde{F}) + W_2(\tilde{F}, \tilde{F}^r) + W_2(\tilde{F}^r, \tilde{F}) + \mathbb{E} [W_1(F^r, \hat{F}_p^r)] \\ &\stackrel{(d)}{\leq} \sqrt{2\sigma^2(1 - \rho^{F, \tilde{F}})} + \sigma - \frac{\sigma}{\sqrt{r}} + \sqrt{\frac{2\sigma^2}{r}(1 - \rho^{F^r, \tilde{F}^r})} + \mathbb{E} [W_1(F^r, \hat{F}_p^r)] \\ &\stackrel{(e)}{\leq} \sqrt{2\sigma^2(1 - \rho^{F, \tilde{F}})} + \sqrt{\frac{2\sigma^2}{r}(1 - \rho^{F^r, \tilde{F}^r})} + \sigma - \frac{\sigma}{\sqrt{r}} + \frac{1}{\sqrt{p}} \int_{\mathbb{R}} \sqrt{F^r(t)(1 - F^r(t))} dt \\ &= \sigma(1 - \frac{1}{\sqrt{r}}) + \frac{1}{\sqrt{p}} \int_{\mathbb{R}} \sqrt{F^r(t)(1 - F^r(t))} dt + \sigma\sqrt{2(1 - \rho^{F, \tilde{F}})} + \sigma\sqrt{(2/r)(1 - \rho^{F^r, \tilde{F}^r})} \end{aligned}$$

Here, (a) and (b) are by triangle inequality, (c) is from the fact that  $W_1 \leq W_2$ , (d) is by Theorem 2 and Equation 2, and (e) is by Proposition 1. We drop the expectation at (b) since  $F$ ,  $F^r$ ,  $\tilde{F}$  and  $\tilde{F}^r$  are not random functions.  $\square$

#### 4.4 Random Sampling

Lastly, we consider the random sampling strategy, where the policymaker selects  $n$  respondents from the population uniformly at random. The analysis in this setting is the most challenging because the resulting subgraph  $\tilde{G}$  induced by the selected respondents is random. Therefore, the number of neighbors each respondent has (i.e., his/her degree) determines the amount of interaction within  $\tilde{G}$ . Suppose that the policymakers select  $n$  respondents uniformly at random and we assume that the sampled respondents follow the average interaction rule. Let the initial beliefs of each of the respondents be a random variable denoted by  $X_1, X_2, \dots, X_n$ , which are drawn i.i.d. from  $\mathcal{F}^*$ . We denote the random variable of the updated belief of each sampled respondent  $i$  to be  $X'_i := \frac{1}{|N_i|+1}(X_i + \sum_{j \in N_i} X_j)$  and the ecdf of the observed belief distribution is given by

$$\hat{F}_n(t) = \frac{1}{n} \sum_{i=1}^n \mathbb{1}(X'_i \leq t).$$

We note that the random variable  $X'_i$  follows a sample mean distribution of  $\mathcal{F}^*$  with size  $d_i + 1$ , where  $d_i := |N_i|$  is the degree of respondent  $i$ . We denote the resulting distribution  $\mathcal{F}^{d_i+1}$ , and we denote the corresponding cdf as  $F^{d_i+1}$ , for all  $i \in \{1, 2, \dots, n\}$ . Then, the mean and standard deviation of  $\mathcal{F}^{d_i+1}$  is  $\mu$  and  $\sigma/(\sqrt{d_i+1})$  respectively. We let  $Y_i(t)$  be the indicator variable  $\mathbb{1}(X'_i \leq t)$ . For a fixed  $t$ ,  $Y_i(t)$  is a Bernoulli random variable, where

$$Y_i(t) = \begin{cases} 1 & \text{w.p. } F^{d_i+1}(t) \\ 0 & \text{w.p. } 1 - F^{d_i+1}(t) \end{cases}$$

Then,  $\mathbb{E}[Y_i(t)] = F^{d_i+1}(t)$  and  $Var(Y_i(t)) = F^{d_i+1}(t)(1 - F^{d_i+1}(t))$ . Before we derive the upper bound of the expected 1-Wasserstein between the ecdf of the observed belief distribution  $\hat{F}_n$  and the cdf of the initial belief distribution  $F$ , we first consider a mixture distribution over the set of cdfs,  $F^{d_1+1}, F^{d_2+1}, \dots, F^{d_n+1}$  with equal weights, where we denote the cdf  $F_n$  as  $\frac{1}{n} \sum_{i=1}^n F^{d_i+1}$ . Then,  $\mathbb{E}[\hat{F}_n(t)] = F_n(t)$ .

Our analysis is complicated by the fact that the interactions can introduce “long range” correlations. Concretely, consider two respondents that are not adjacent to each other but share a common neighbor. Even though the respondents do not directly interact with each other, the presence of a common neighbor induces an indirect form of interaction and their updated beliefs are correlated. As such, a key part of our analysis is to bound the correlation introduced by these “long range” connections. In what follows, for every respondent  $i$ , we consider the set of neighbors, denoted by  $N_i$  as well as the set of vertices that are two hops from  $i$ , denoted by  $M_i$ . To capture this correlation, we make use of a 2-star graph, as defined below to quantify the number of vertices that are 2-hops away from a given vertex.

**Definition 1.** *A 2-star graph is a graph that has 3 vertices and 2 edges, where the central vertex is adjacent to 2 leaf vertices.*

Given the adjacency matrix  $A$  of the resulting subgraph after sampling, the  $(r, s)$ -entry of  $A^2$  gives the number of 2 hops from respondent  $r$  to  $s$ . Hence, using  $A$  and  $A^2$ , we define the

indicator variable  $M_{r,s}$ , where respondent  $s$  is at most 2 hops from  $r$ , as follows,

$$M_{r,s} = \begin{cases} 1 & \text{if } A_{r,s} + A_{r,s}^2 \geq 1 \\ 0 & \text{otherwise} \end{cases}$$

where  $A_{r,s}$  and  $A_{r,s}^2$  are the  $(r,s)$ -entry of  $A$  and  $A^2$  respectively. We also make the following assumption to obtain an upper bound on the number of common neighbors that two sampled respondents share. This allows us to achieve a tighter bound, as illustrated in the deferred analysis.

**Assumption 1.** *Given a graph  $G(V, E)$ , we assume that there are at most  $2n(\langle d \rangle + \langle d \rangle^2)$  “long range” connections, i.e.,  $\sum_{r \neq s} M_{r,s} \leq 2n(\langle d \rangle + \langle d \rangle^2)$ , where  $\langle d \rangle$  is the average degree of  $G$ .*

We substantiate the assumption using the Erdős-Renyi random graph model,  $\mathcal{R}(|V|, p)$  in the following claim.

**Claim 1.** *Let  $G(V, E)$  be a graph where the edges are formed according to the Erdős-Renyi random graph model  $\mathcal{R}(|V|, p)$ . Let  $\mathbf{L}_v$  be the random variable for the number of vertices that are within 2 hops away from a given vertex  $v \in V$ . Then, for all vertices in  $G$ , Assumption 1 holds with probability*

$$\mathbb{P} \left( \bigcap_{v \in V} (\mathbf{L}_v \leq 2\langle d \rangle + 2\langle d \rangle^2) \right) \gtrsim 1 - \frac{2}{|V|p^2}.$$

*Proof.* As a proof sketch, for a given vertex  $v$ , we first provide a probabilistic bound on  $|N_v|$  by considering the degree of  $v$ . Then, we bound  $|M_v|$  using 2-star graphs with  $v$  as a leaf vertex. Lastly, we will invoke the union bound to prove the claim.

*Bounding  $|N_v|$ :* For a given vertex  $v$ , let  $\mathbf{D}_v$  be the degree of  $v$ . Under an Erdős-Renyi random graph model,  $\mathcal{R}(|V|, p)$ ,  $\mathbf{D}_v$  is the sum of  $|V|-1$  independent Bernoulli random variables with success probability  $p$ . Since the degree of any vertex under  $\mathcal{R}(|V|, p)$  follows the same binomial distribution, the average degree  $\langle d \rangle$  of the graph is  $(|V|-1)p$ , which is equivalent to  $\mathbb{E}[\mathbf{D}_v]$ . Hence, the tail probability of  $\mathbf{D}_v$  exceeding twice the average degree, is given as

$$\mathbb{P}(\mathbf{D}_v \geq 2\mathbb{E}[\mathbf{D}_v]) = \mathbb{P}(\mathbf{D}_v - \mathbb{E}[\mathbf{D}_v] \geq \mathbb{E}[\mathbf{D}_v]) \stackrel{(a)}{\leq} \exp\left(-\frac{2\mathbb{E}[\mathbf{D}_v]^2}{|V|-1}\right) = \exp(-2p^2(|V|-1))$$

where (a) is by the Hoeffding’s inequality.

*Bounding  $|M_v|$ :* To bound the number of vertices that are exactly 2-hops away from  $v$ , we consider the number of 2-stars with  $v$  as a leaf vertex. We denote  $\mathbf{D}_{2v}$  as the random variable for the number of 2-stars with  $v$  as a leaf vertex. Then, the expected number of 2-stars is given as

$$\mathbb{E}[\mathbf{D}_{2v}] = (|V|-1)(|V|-2)p^2 \approx \langle d \rangle^2$$

The random variable  $\mathbf{D}_{2v}$  is represented as  $\sum_j \mathbf{1}_{\tau_j}$ , where  $\tau_j$  is the event that the  $j$ -th triple of vertices  $(v_{j1}, v_{j2}, v_{j3})$ , form a 2-star with  $v$  as a leaf vertex. Then,  $\mathbb{E}[(\mathbf{D}_{2v})^2]$  is given as,

$$\mathbb{E}[(\mathbf{D}_{2v})^2] = \mathbb{E}\left[\left(\sum_j \mathbf{1}_{\tau_j}\right)^2\right] = \mathbb{E}\left[\sum_j \mathbf{1}_{\tau_j}\right] + \sum_{j \neq k} \mathbb{E}\left[\mathbf{1}_{\tau_j} \mathbf{1}_{\tau_k}\right]$$

As  $\mathbb{E}[\mathbf{1}_{\tau_j} \mathbf{1}_{\tau_k}] = \mathbb{P}(\mathbf{1}_{\tau_j} \cap \mathbf{1}_{\tau_k})$  is the probability that both triples  $j$  and  $k$  have a 2-star with  $v$  as a leaf vertex. If  $\tau_j \cap \tau_k = v$ , then  $\mathbb{P}(\tau_j \cap \tau_k) = p^4$ ; if  $\tau_j$  and  $\tau_k$  have 2 common vertices, including  $v$  and no common edge, then  $\mathbb{P}(\tau_j \cap \tau_k) = p^4$  and if  $\tau_j$  and  $\tau_k$  have 2 common vertices, including  $v$  and 1 common edge, then  $\mathbb{P}(\tau_j \cap \tau_k) = p^3$ . The total number of the pairs of triples  $j$  and  $k$  with  $v$  as a common vertex is  $4 \binom{|V|-1}{2} \binom{|V|-3}{2}$ , with 2 common vertices including  $v$  and a common edge is  $2 \binom{|V|-1}{2} (|V|-3)$  and with two common vertices including  $v$  and no common edge is  $4 \binom{|V|-1}{2} (|V|-3)$ . Summing, we have

$$\sum_{j \neq k} \mathbb{E}[\mathbf{1}_{\tau_j} \mathbf{1}_{\tau_k}] = \sum_{j \neq k} \mathbb{P}(\mathbf{1}_{\tau_j} \cap \mathbf{1}_{\tau_k}) = 4 \binom{|V|-1}{2} \binom{|V|-3}{2} p^4 + 2 \binom{|V|-1}{2} (|V|-3) p^3 + 4 \binom{|V|-1}{2} (|V|-3) p^4$$

Using the facts that  $\binom{|V|-1}{2} \sim \binom{|V|-3}{2} \sim \frac{|V|^2}{2}$  and  $|V|-3 \sim |V|$ , we find that  $\sum_{j \neq k} \mathbb{E}[\mathbf{1}_{\tau_j} \mathbf{1}_{\tau_k}] = (1 + o(1)) \mathbb{E}[\mathbf{D}_{2v}]^2$ , for any given vertex  $v$ . Then, the tail probability of  $\mathbf{D}_{2v}$  exceeding twice its mean is given as

$$\begin{aligned} \mathbb{P}(\mathbf{D}_{2v} \geq 2\mathbb{E}[\mathbf{D}_{2v}]) &\stackrel{(a)}{\leq} \frac{\text{Var}(\mathbf{D}_{2v})}{\mathbb{E}[\mathbf{D}_{2v}]^2} \\ &= \frac{\mathbb{E}[(\mathbf{D}_{2v})^2] - \mathbb{E}[\mathbf{D}_{2v}]^2}{\mathbb{E}[\mathbf{D}_{2v}]^2} \\ &= \frac{\mathbb{E}[\mathbf{D}_{2v}] + \sum_{j \neq k} \mathbb{E}[\mathbf{1}_{\tau_j} \mathbf{1}_{\tau_k}] - \mathbb{E}[\mathbf{D}_{2v}]^2}{\mathbb{E}[\mathbf{D}_{2v}]^2} \\ &= \frac{1}{\mathbb{E}[\mathbf{D}_{2v}]} + o(1) \\ &= \frac{1}{(|V|-1)(|V|-2)p^2} + o(1) \end{aligned}$$

where (a) is by the Chebyshev inequality. Combining both probabilities with the union bound and using the fact that  $|V|-2 \sim |V|-1 \sim |V|$ , we have

$$\begin{aligned} \mathbb{P}(\bigcap_{v \in V} (\mathbf{L}_v \leq 2(\langle d \rangle + \langle d \rangle^2))) &\stackrel{(a)}{\geq} 1 - \sum_{v \in V} \mathbb{P}(\mathbf{D}_v + \mathbf{D}_{2v} \geq 2(\langle d \rangle + \langle d \rangle^2)) \\ &\stackrel{(b)}{\geq} 1 - \sum_{v \in V} \mathbb{P}(\mathbf{D}_v \geq 2\langle d \rangle) - \sum_{v \in V} \mathbb{P}(\mathbf{D}_{2v} \geq 2\langle d \rangle^2) \\ &= 1 - |V| \exp(-2p^2(|V|-1)) - \frac{|V|}{(|V|-1)(|V|-2)p^2} - o(1) \\ &\gtrsim 1 - \frac{2}{|V|p^2} \end{aligned}$$

where (a) and (b) are by the union bound. Then, Assumption 1 holds with high probability for sufficiently large  $|V|$ .  $\square$

Claim 1 shows that for a graph  $G(V, E)$ , there are at most  $2n(\langle d \rangle + \langle d \rangle^2)$  “long range” connections with high probability. This analysis suggests that Assumption 1 is reasonable. In what follows, we provide an upper bound of the expected 1-Wasserstein distance between  $\hat{F}_n$  and  $F$  supposing Assumption 1 holds. We note that there are two elements of randomness, specifically, the sampling strategy and their initial beliefs, which are independent of each other. Hence, to quantify the expected 1-Wasserstein distance, we invoke the law of iterated expectation. We first consider the “inner” expectation after  $n$  respondents have been selected uniformly at random and state the following proposition for the upper bound. In the following, we let  $\tilde{F}$  and  $\tilde{F}^{d_i+1}$  be the cdfs of the normal distributions  $N(\mu, \sigma^2)$  and  $N(\mu, \frac{\sigma^2}{d_i+1})$  for  $i \in [n]$ .

**Proposition 3.** *Given the resulting subgraph  $\tilde{G}$  obtained by randomly selecting  $n$  respondents. Suppose Assumption 1 holds. Then the expected 1-Wasserstein distance between the ecdf of the observed belief distribution  $\hat{F}_n$  and the cdf of the initial belief distribution  $F$  has the following upper bound,*

$$\begin{aligned} \mathbb{E} \left[ W_1(\hat{F}_n, F) \right] &\leq \frac{1}{n} \int_{\mathbb{R}} \sqrt{\sum_{i=1}^n F^{d_i+1}(t)(1 - F^{d_i+1}(t))} dt \\ &\quad + \sigma \sqrt{2(1 - \rho^{F, \tilde{F}})} + \sigma \left( 1 - \frac{1}{n} \sum_{i=1}^n \frac{1}{\sqrt{d_i + 1}} \right) + \frac{\sigma}{n} \sum_{i=1}^n \sqrt{\frac{2(1 - \rho^{F^{d_i+1}, \tilde{F}^{d_i+1}})}{d_i + 1}} \\ &\quad + \frac{O(\langle d \rangle)}{\sqrt{n}} \end{aligned}$$

where  $\rho^{F, \tilde{F}}$  and  $\rho^{F^{d_i+1}, \tilde{F}^{d_i+1}}$  are the respective Pearson correlation of the points in the quantile-quantile plot of  $F$  and  $\tilde{F}$ , and  $F^{d_i+1}$  and  $\tilde{F}^{d_i+1}$  for  $i \in [n]$  and  $\langle d \rangle$  is the average degree of  $\tilde{G}$ .

*Proof.* Using a similar proof technique in Proposition 2, we first obtain the following inequality,

$$\begin{aligned} \mathbb{E} \left[ W_1(\hat{F}_n, F) \right] &\stackrel{(a)}{\leq} \mathbb{E} \left[ W_1(\hat{F}_n, F_n) \right] + \mathbb{E} \left[ W_1(F_n, F) \right] \\ &\stackrel{(b)}{\leq} \int_{\mathbb{R}} \sqrt{\text{Var}(\hat{F}_n(t))} dt + W_1(F_n, F) \end{aligned}$$

where (a) is by triangle inequality, (b) is by Proposition 1 as  $\mathbb{E} \left[ \hat{F}_n(t) \right] = F_n(t)$ . Since  $F_n$  and  $F$  are not random functions, we drop the expectation in the second term.

In the variance term, we note that there is a non-zero probability that the sampled respondents know each other or have common neighbors. Hence, there are covariance terms and the indicator variable  $M_{r,s}$  detects whether sampled respondents  $r$  and  $s$  share an edge or a common neighbor. For a fixed  $t$ , we have,

$$\begin{aligned} \text{Var}(\hat{F}_n(t)) &= \frac{1}{n^2} \left( \sum_{i=1}^n \text{Var}(Y_i(t)) + \sum_{r \neq s} \text{Cov}(Y_r(t), Y_s(t)) \right) \\ &\stackrel{(a)}{\leq} \frac{1}{n^2} \left( \sum_{i=1}^n F^{d_i+1}(t)(1 - F^{d_i+1}(t)) + \sum_{r \neq s} M_{r,s} \sqrt{\text{Var}(Y_r(t))\text{Var}(Y_s(t))} \right) \\ &\stackrel{(b)}{\leq} \frac{1}{n^2} \left( \sum_{i=1}^n F^{d_i+1}(t)(1 - F^{d_i+1}(t)) + C_t(\langle d \rangle + \langle d \rangle^2)n \right) \end{aligned}$$

where (a) is by Cauchy-Schwarz inequality, (b) is by Assumption 1 and  $C_t = \max_i \{F^{d_i+1}(t)(1 - F^{d_i+1}(t))\}$ . By substituting the variance term into the integral, we have

$$\begin{aligned} \int_{\mathbb{R}} \sqrt{\text{Var}(\hat{F}_n(t))} dt &= \frac{1}{n} \int_{\mathbb{R}} \sqrt{\sum_{i=1}^n F^{d_i+1}(t)(1 - F^{d_i+1}(t)) + C_t(\langle d \rangle + \langle d \rangle^2)n} dt \\ &\leq \frac{1}{n} \int_{\mathbb{R}} \sqrt{\sum_{i=1}^n F^{d_i+1}(t)(1 - F^{d_i+1}(t))} dt + \frac{\sqrt{(1 + \frac{1}{\langle d \rangle})\langle d \rangle^2 n}}{n} \int_{\mathbb{R}} \sqrt{C_t} dt \\ &= \frac{1}{n} \int_{\mathbb{R}} \sqrt{\sum_{i=1}^n F^{d_i+1}(t)(1 - F^{d_i+1}(t))} dt + \frac{O(\langle d \rangle)}{\sqrt{n}} \end{aligned}$$

We note that splitting the square-root term may be unnecessary, but it helps to improve the “visibility” of the contribution of the sample size term and the term representing the presence



of the shared edges and common neighbors to the upper bound. For the second term, we use a similar technique in Proposition 2, which we then obtain the following upper bound,

$$\begin{aligned}
W_1(F_n, F) &= W_1\left(\frac{\sum_{i=1}^n F^{d_i+1}}{n}, \frac{\sum_{i=1}^n F}{n}\right) \\
&\stackrel{(a)}{\leq} W_1\left(\frac{\sum_{i=1}^n F^{d_i+1}}{n}, \frac{\sum_{i=1}^n \tilde{F}^{d_i+1}}{n}\right) + W_1\left(\frac{\sum_{i=1}^n \tilde{F}^{d_i+1}}{n}, \frac{\sum_{i=1}^n \tilde{F}}{n}\right) + W_1\left(\frac{\sum_{i=1}^n \tilde{F}}{n}, \frac{\sum_{i=1}^n F}{n}\right) \\
&\stackrel{(b)}{\leq} \frac{1}{n} \sum_{i=1}^n W_1(F^{d_i+1}, \tilde{F}^{d_i+1}) + W_1(\tilde{F}^{d_i+1}, \tilde{F}) + W_1(\tilde{F}, F) \\
&\stackrel{(c)}{\leq} \sigma \sqrt{2(1 - \rho^{F, \tilde{F}})} + \sigma \left(1 - \frac{1}{n} \sum_{i=1}^n \frac{1}{\sqrt{d_i+1}}\right) + \frac{\sigma}{n} \sum_{i=1}^n \sqrt{\frac{2(1 - \rho^{F^{d_i+1}, \tilde{F}^{d_i+1}})}{d_i+1}}
\end{aligned}$$

Here, (a) and (b) are by triangle inequality, and (c) is using a similar technique in Proposition 2. Combining the two terms, we have

$$\begin{aligned}
\mathbb{E}\left[W_1(\hat{F}_n, F)\right] &\leq \frac{1}{n} \int_{\mathbb{R}} \sqrt{\sum_{i=1}^n F^{d_i+1}(t)(1 - F^{d_i+1}(t))} dt \\
&\quad + \sigma \sqrt{2(1 - \rho^{F, \tilde{F}})} + \sigma \left(1 - \frac{1}{n} \sum_{i=1}^n \frac{1}{\sqrt{d_i+1}}\right) + \frac{\sigma}{n} \sum_{i=1}^n \sqrt{\frac{2(1 - \rho^{F^{d_i+1}, \tilde{F}^{d_i+1}})}{d_i+1}} \\
&\quad + \frac{O(\langle d \rangle)}{\sqrt{n}}
\end{aligned}$$

□

We distil two effects from the bounds stated in Proposition 3. The term in the first row can be interpreted as the *sample size effect* while the other terms can be interpreted as the deviation in the policy belief, i.e., *interaction effect*. Intuitively, the interaction effect can be attributed to the extent of interaction among respondents and the number of respondents one interacts with, which are respectively described by the terms in the second and third rows on the RHS. Through this bound, we illustrate the tradeoff between the sample size effect and the interaction effect. Although the policymakers could weaken the sample size effect by increasing the sampling size while working within their constraints, they would have to discern and quantify the estimation performance loss due to the possible interaction effect.

As Proposition 3 is based on a given resulting subgraph after sampling, the policymakers might not know the entire population network and the topology of this network can affect the resulting subgraph through the sampling process. Since the resulting subgraph varies across different samples of  $n$  respondents, this implies that the size of the sample mean distribution  $\mathcal{F}^{d_i+1}$ , for each respondent  $i$ , is dependent on the resulting subgraph. By conditioning on the set of sampled respondents, we fix the subgraph  $\tilde{G}$  and we apply the result from Proposition 3. Hence, using the law of iterated expectation, we have the following corollary.

**Corollary 1.** *Given the population graph  $G(P, E)$ , the expected 1-Wasserstein distance between the ecdf  $\hat{F}_n$  and the cdf of the initial belief distribution  $F$  is given as*

$$\mathbb{E}[W_1(\hat{F}_n, F)] = \mathbb{E}\left[\mathbb{E}\left[W_1(\hat{F}_n, F) | \tilde{G}\right]\right]$$

where the inner expectation is from Proposition 3, which we then take the expectation over all

possible resulting subgraphs that consist of  $n$  respondents.

As a note, we provide Corollary 1 to address the context of the problem. Explicitly stating the full expectation is rather convoluted and it doesn't provide additional insights, so we provide the expansion in Appendix B. However, the bounds are concentrated around the expected degree of the sampled respondent in the resulting subgraph, which depends on population size  $|V|$ , sample size  $n$  and the degree of each respondent in the population.

## 5 Effects of Interactions and Graphical Network

In this section, we explore a number of extensions of the results in the previous section. First, we investigate how the topology of the relationship network between respondents affects our estimates derived earlier. Second, we explore alternative interaction contexts. Previously, we plainly assumed that each respondent weighs the opinion of all other respondents that he or she knows, including his or her own, equally. However, in many real-life situations, respondents listen to their neighbors to different extents, where they would adopt the beliefs of some more strongly than others or stick to their own beliefs more firmly. We explore how alternative interaction contexts affect our results.

### 5.1 Simple illustrative networks

In this subsection, we illustrate how the Wasserstein distance changes analytically as the size of the resulting subgraph increases, assuming that the sampled respondents follow the average interaction rule. This allows the policymakers to quantify the *first-order effect* on the deviation as edges begin to emerge in the subgraph.

Suppose a population network  $G_1(P, \{e\})$ , where a pair of respondents share edge  $e$  while the others are isolated and policymakers select  $n$  respondents from the population uniformly at random. Let the initial beliefs of each of the respondents be a random variable denoted by  $X_1, X_2, \dots, X_n$ , which are drawn i.i.d. from  $\mathcal{F}^*$ . Without loss of generality, we assign the random variables  $X_1$  and  $X_2$  to the respondents who know each other.

There are two scenarios after the selection; either the pair of respondents who know each other is selected or otherwise. In the former scenario, we let  $\hat{F}_{n,1}$  and  $\hat{F}'_{n,1}$  be the ecdf of the belief distributions before and after the interaction respectively. Then, the ecdf of the observed belief distribution  $\hat{F}'_{n,1}$  is given as

$$\hat{F}'_{n,1}(t) = \frac{2\mathbf{1}(\frac{X_1+X_2}{2} \leq t) + \sum_{i=3}^n \mathbf{1}(X_i \leq t)}{n}$$

We provide the expected 1-Wasserstein distance between  $\hat{F}_{n,1}$  and  $\hat{F}'_{n,1}$  in the following proposition.

**Proposition 4.** *The expected 1-Wasserstein distance between  $\hat{F}_{n,1}$  and  $\hat{F}'_{n,1}$  is given as*

$$\mathbb{E} \left[ W_1(\hat{F}_{n,1}, \hat{F}'_{n,1}) \right] = \frac{2}{n} \int_{\mathbb{R}} F(t)(1 - F(t))dt.$$

*Proof.*

$$\begin{aligned} \mathbb{E} \left[ W_1(\hat{F}_{n,1}, \hat{F}'_{n,1}) \right] &= \mathbb{E} \left[ \int_{\mathbb{R}} |\hat{F}_{n,1}(t) - \hat{F}'_{n,1}(t)| dt \right] \\ &\stackrel{(a)}{=} \mathbb{E} \left[ \int_{\min\{X_1, X_2\}}^{\max\{X_1, X_2\}} \frac{1}{n} dt \right] \\ &\stackrel{(b)}{=} \frac{1}{n} \int_{\mathbb{R}} \mathbb{P}(\min\{X_1, X_2\} \leq t \leq \max\{X_1, X_2\}) dt \\ &= \frac{1}{n} \int_{\mathbb{R}} 1 - \mathbb{P}(\min\{X_1, X_2\} \geq t) - \mathbb{P}(\max\{X_1, X_2\} \leq t) dt \\ &= \frac{2}{n} \int_{\mathbb{R}} F(t)(1 - F(t))dt \end{aligned}$$

We note that (a) comes from the fact that the ecdfs  $\hat{F}_{n,1}$  and  $\hat{F}'_{n,1}$  are the same on the intervals,  $(-\infty, X_1)$  and  $(X_2, \infty)$  as the number of people having a belief in these intervals does not change and (b) comes from the fact that there is one less person who has a belief between  $X_1$  and  $\frac{X_1+X_2}{2}$  and there is one more person who has a belief between  $\frac{X_1+X_2}{2}$  and  $X_2$ .  $\square$

For the latter scenario, there are no edges in the resulting subgraph, which implies no interaction between the sampled respondents. Hence, the sample is essentially an independent set sample. So, the ecdf of the observed belief distribution when the pair of respondents is not selected, denoted by  $\hat{F}'_{n,0}$ , is given as,

$$\hat{F}'_{n,0}(t) = \frac{\sum_{i=1}^n \mathbf{1}(X_i \leq t)}{n}$$

We note that the ecdfs  $\hat{F}'_{n,0}$  and  $\hat{F}_{n,1}$  are the same as there is no interaction among respondents and the ecdf  $\hat{F}'_{n,0}$  is an estimate of the cdf  $F$ . By computing the upper bound of the expected 1-Wasserstein distance between the initial and empirically observed belief distributions, we illustrate the first-order interaction effect on the deviation as edges start to emerge.

**Proposition 5.** *Given the population network  $G_1$  and  $n$  respondents are selected uniformly at random, the expected 1-Wasserstein distance between the ecdf of the observed belief distribution  $\hat{H}_n$  and the cdf of the initial belief distribution  $F$  has the following upper bound,*

$$\mathbb{E} \left[ W_1(\hat{H}_n, F) \right] \leq \frac{2p_1}{n} \int_{\mathbb{R}} F(t)(1 - F(t))dt + \frac{1}{\sqrt{n}} \int_{\mathbb{R}} \sqrt{F(t)(1 - F(t))} dt$$

where  $p_1$  is the probability of including the only edge in  $G_1$  in the resulting subgraph.

*Proof.* First, we note the probability that the resulting subgraph contains the only edge in  $G_1$ , which is given as

$$p_1 = \binom{|P|-2}{n-2} / \binom{|P|}{n}$$

As the ecdf  $\hat{H}_n$  is a random function that takes on different ecdfs based on the number of edges in the resulting subgraph, then the ecdf  $\hat{H}_n(t)$  is given as

$$\hat{H}_n(t) = p_0 \hat{F}'_{n,0}(t) + p_1 \hat{F}'_{n,1}(t)$$

where  $p_0 = 1 - p_1$ . Since the ecdfs  $\hat{F}'_{n,0}$  and  $\hat{F}_{n,1}$  are the same, the expected 1-Wasserstein distance is upper-bounded by

$$\begin{aligned}
\mathbb{E} \left[ W_1(\hat{H}_n, F) \right] &= \mathbb{E} \left[ \int_{\mathbb{R}} |\hat{H}_n(t) - \hat{F}'_{n,0}(t) + \hat{F}'_{n,0}(t) - F(t)| dt \right] \\
&= \mathbb{E} \left[ \int_{\mathbb{R}} |p_0 \hat{F}'_{n,0}(t) + p_1 \hat{F}'_{n,1}(t) - \hat{F}'_{n,0}(t) + \hat{F}'_{n,0}(t) - F(t)| dt \right] \\
&\leq \mathbb{E} \left[ \int_{\mathbb{R}} |p_1 \hat{F}'_{n,1}(t) - p_1 \hat{F}'_{n,0}(t)| dt + \int_{\mathbb{R}} |\hat{F}'_{n,0}(t) - F(t)| dt \right] \\
&= p_1 \mathbb{E} \left[ \int_{\mathbb{R}} |\hat{F}'_{n,1}(t) - \hat{F}'_{n,0}(t)| dt \right] + \mathbb{E} \left[ \int_{\mathbb{R}} |\hat{F}'_{n,0}(t) - F(t)| dt \right] \\
&= p_1 \mathbb{E} \left[ \int_{\min\{X_1, X_2\}}^{\max\{X_1, X_2\}} \frac{1}{n} dt \right] + \mathbb{E} \left[ \int_{\mathbb{R}} |\hat{F}'_{n,0}(t) - F(t)| dt \right] \\
&\stackrel{(a)}{=} \frac{2p_1}{n} \int_{\mathbb{R}} F(t)(1 - F(t)) dt + \mathbb{E} \left[ W_1(\hat{F}'_{n,0}, F) \right] \\
&\stackrel{(b)}{\leq} \frac{2p_1}{n} \int_{\mathbb{R}} F(t)(1 - F(t)) dt + \frac{1}{\sqrt{n}} \int_{\mathbb{R}} \sqrt{F(t)(1 - F(t))} dt
\end{aligned}$$

where (a) is by Proposition 4 and (b) is by Proposition 1.  $\square$

Next, we increase the number of disjoint edges in the population network. Suppose a population network  $G_m(P, E_m)$  with  $m$  disjoint edges, where  $m \leq \lfloor \frac{|P|}{2} \rfloor$  and policymakers select  $n$  respondents from the population uniformly at random. Let the initial beliefs of each of the respondents be a random variable denoted by  $X_1, X_2, \dots, X_n$ , which are drawn i.i.d. from  $\mathcal{F}^*$ . Without loss of generality, we assign the random variables  $X_1, X_2, \dots, X_{2k}$  to the respondents who share a tie. For the case where  $k$  connected pairs of respondents are included in the sample, for  $k \leq m$ , let  $\hat{F}_{n,k}$  and  $\hat{F}'_{n,k}$  be the ecdf of the belief distributions before and after the interaction respectively. Then, we have the following result.

**Proposition 6.** *The expected 1-Wasserstein distance between  $F_{n,k}$  and  $F'_{n,k}$  has the following upper bound,*

$$\mathbb{E} \left[ W_1(F_{n,k}, F'_{n,k}) \right] \leq \frac{k}{n} \int_{\mathbb{R}} 1 - (1 - F(t))^{2k} - F(t)^{2k} dt$$

*Proof.*

$$\begin{aligned}
\mathbb{E} \left[ W_1(\hat{F}_{n,k}, \hat{F}'_{n,k}) \right] &= \mathbb{E} \left[ \int_{\mathbb{R}} |\hat{F}_{n,k}(t) - \hat{F}'_{n,k}(t)| dt \right] \\
&\stackrel{(a)}{=} \mathbb{E} \left[ \int_{\min_{i \in [2k]} \{X_i\}}^{\max_{j \in [2k]} \{X_j\}} \frac{k}{n} dt \right] \\
&\stackrel{(b)}{\leq} \frac{k}{n} \int_{\mathbb{R}} \mathbb{P} \left( \min_{i \in [2k]} \{X_i\} \leq t \leq \max_{j \in [2k]} \{X_j\} \right) dt \\
&= \frac{k}{n} \int_{\mathbb{R}} 1 - \mathbb{P} \left( \min_{i \in [2k]} \{X_i\} \geq t \right) - \mathbb{P} \left( \max_{i \in [2k]} \{X_i\} \leq t \right) dt \\
&= \frac{k}{n} \int_{\mathbb{R}} 1 - (1 - F(t))^{2k} - F(t)^{2k} dt
\end{aligned}$$

We note that (a) comes from the fact that the ecdf of  $\hat{F}_{n,k}$  and  $\hat{F}'_{n,k}$  are the same when in the intervals,  $(-\infty, \min_{i \in [2k]} \{X_i\})$  and  $(\max_{j \in [2k]} \{X_j\}, \infty)$  as the number of people having a belief in these intervals does not change and (b) comes from the fact that there is a difference in belief for at most  $k$  people within the interval  $[\min_{i \in [2k]} \{X_i\}, \max_{j \in [2k]} \{X_j\}]$ .  $\square$

Similar to the single edge case, we can compute the upper bound of the expected 1-Wasserstein distance between the initial and empirically observed belief distributions.

**Proposition 7.** *Given the population network  $G_m$  and  $n$  respondents are selected uniformly at random, the expected 1-Wasserstein distance between the ecdf of the observed belief distribution  $\hat{H}_n$  and the cdf of the initial belief distribution  $F$  has the following upper bound,*

$$\mathbb{E} \left[ W_1(\hat{H}_n, F) \right] \leq \sum_{k=1}^m \frac{kp_k}{n} \int_{\mathbb{R}} 1 - (1 - F(t))^{2k} - F(t)^{2k} dt + \frac{1}{\sqrt{n}} \int_{\mathbb{R}} \sqrt{F(t)(1 - F(t))} dt$$

where  $p_k$  is the probability that the resulting subgraph contains  $k$  edges, for  $k \in \{1, 2, \dots, m\}$ .

*Proof.* As the ecdf  $\hat{H}_n$  is a random function that takes on different ecdfs based on the number of edges in the resulting subgraph, then the ecdf  $\hat{H}_n(t)$  is given as

$$\hat{H}_n(t) = \sum_{k=0}^m p_k \hat{F}'_{n,k}(t)$$

where  $p_k$  is the probability of having  $k$  edges in the resulting subgraph, for  $k \in \{0, 1, \dots, m\}$  and the ecdf  $\hat{F}'_{n,k}(t)$  is given as

$$\frac{2 \sum_{j=0}^k \mathbb{1} \left( \frac{X_{2j-1} + X_{2j}}{2} \leq t \right) + \sum_{i=2k+1}^n \mathbb{1}(X_i \leq t)}{n}$$

We note that the ecdf  $\hat{F}'_{n,0}$  is an estimate of the cdf  $F$ . Since the ecdfs  $\hat{F}'_{n,0}$  and  $\hat{F}'_{n,k}$ , for  $k \in \{0, 1, \dots, m\}$ , are the same as there are no interactions between respondents, the expected 1-Wasserstein distance is upper-bounded by

$$\begin{aligned} \mathbb{E} \left[ W_1(\hat{H}_n, F) \right] &= \mathbb{E} \left[ \int_{\mathbb{R}} |\hat{H}_n(t) - \hat{F}'_{n,0}(t) + \hat{F}'_{n,0}(t) - F(t)| dt \right] \\ &= \mathbb{E} \left[ \int_{\mathbb{R}} \left| \sum_{k=0}^m p_k \hat{F}'_{n,k}(t) - \hat{F}'_{n,0}(t) + \hat{F}'_{n,0}(t) - F(t) \right| dt \right] \\ &\stackrel{(a)}{\leq} \sum_{k=1}^m p_k \mathbb{E} \left[ \int_{\mathbb{R}} |\hat{F}'_{n,k}(t) - \hat{F}'_{n,0}(t)| dt \right] + \mathbb{E} \left[ \int_{\mathbb{R}} |\hat{F}'_{n,0}(t) - F(t)| dt \right] \\ &\stackrel{(b)}{\leq} \sum_{k=1}^m \frac{kp_k}{n} \int_{\mathbb{R}} 1 - (1 - F(t))^{2k} - F(t)^{2k} dt + \mathbb{E} \left[ W_1(\hat{F}'_{n,0}, F) \right] \\ &\stackrel{(c)}{\leq} \sum_{k=1}^m \frac{kp_k}{n} \int_{\mathbb{R}} 1 - (1 - F(t))^{2k} - F(t)^{2k} dt + \frac{1}{\sqrt{n}} \int_{\mathbb{R}} \sqrt{F(t)(1 - F(t))} dt \end{aligned}$$

where (a) is by Fubini's Theorem and triangle inequality, (b) is by Proposition 6 and (c) is by Proposition 1 respectively.  $\square$

The results from Propositions 5 and 7 shed light on how the presence of minimal edges in the sample size could affect the deviation in the distributions and provide a simpler illustration of Proposition 3 in the earlier section.

## 5.2 Directed Networks

In this subsection, we consider directed network structures. These structures mimic the situation where there are influencers and followers in the society and the followers would update their beliefs with reference to those of the influencers. To effectively model this phenomenon, we consider the random sampling strategy. We note that the independent set sampling strategy is

ineffective in modeling this phenomenon as this strict sampling strategy neglects the directionality in the network. By assuming that the sampled respondents follow the average interaction rule, the update depends on the out-degree of each node, as denoted by  $d^o$ , i.e. the number of neighbors that each respondent listens to in the resulting subgraph.

Suppose that the policymakers select  $n$  respondents from the population uniformly at random. Let the initial beliefs of each of the respondents be a random variable denoted by  $X_1, X_2, \dots, X_n$ , which are drawn i.i.d. from  $\mathcal{F}^*$ . We denote the random variable of the updated belief of each sampled respondent  $i$  to be  $X_i^d := \frac{1}{d_i^o+1}(X_i + \sum_{j \in N_i^d} X_j)$ , where  $N_i^d$  is the set of indices (vertices) within  $\tilde{G}$  that has a directed relationship with respondent  $i$ , i.e.,  $d_i^o = |N_i^d|$ . Then, the ecdf of the observed belief distribution,  $\hat{F}_n(t)$  is given as

$$\hat{F}_n(t) = \frac{1}{n} \sum_{i=1}^n \mathbb{1}(X_i^d \leq t)$$

We note that the random variable  $X_i^d$  follows a sample mean distribution of  $\mathcal{F}^*$  with size  $d_i^o+1$ . We denote the resulting distribution  $\mathcal{F}^{d_i^o+1}$ , and we denote the corresponding cdf as  $F^{d_i^o+1}$ , for all  $i \in \{1, 2, \dots, n\}$ . Then, the mean and standard deviation of  $\mathcal{F}^{d_i^o+1}$  is  $\mu$  and  $\sigma/(\sqrt{d_i^o+1})$  respectively. We let  $Y_i^d(t)$  be the indicator variable  $\mathbb{1}(X_i^d \leq t)$ . For a fixed  $t$ ,  $Y_i^d(t)$  is a Bernoulli random variable, where

$$Y_i^d(t) = \begin{cases} 1 & \text{w.p. } F^{d_i^o+1}(t) \\ 0 & \text{w.p. } 1 - F^{d_i^o+1}(t) \end{cases}$$

Then,  $\mathbb{E}[Y_i^d(t)] = F^{d_i^o+1}(t)$  and  $\text{Var}(Y_i^d(t)) = F^{d_i^o+1}(t)(1 - F^{d_i^o+1}(t))$ . We note that the analysis of the expected 1-Wasserstein distance for the directed networks is analogous to the analysis in Subsection 4.4. Similar to the earlier analysis, we also construct a similar indicator variable  $M_{r,s}^d$  to detect directed relationships and common directed neighbors, as follows,

$$M_{r,s}^d = \begin{cases} 1 & \text{if } A_{r,s} + \sum_{t \neq r,s} A_{t,r} A_{t,s} \geq 1 \\ 0 & \text{otherwise} \end{cases}$$

where  $A_{r,s}$  is the  $(r, s)$ -entry of the adjacency matrix  $A$ .

**Assumption 2.** *Using a similar analysis involving Assumption 1 and Claim 1 in the earlier section, we assume that  $\sum_{r \neq s} M_{r,s}^d \leq 2n(\langle d^o \rangle + \langle d^o \rangle^2)$ , where  $\langle d^o \rangle$  is the average out-degree in the population network  $G^d$ .*

In the following, we let  $\tilde{F}$  and  $\tilde{F}^{d_i^o+1}$  be the cdfs of the normal distributions  $N(\mu, \sigma^2)$  and  $N(\mu, \frac{\sigma^2}{d_i^o+1})$  for  $i \in [n]$ .

**Corollary 2.** *Given the directed resulting subgraph  $\tilde{G}^d$  obtained by randomly selecting  $n$  respondents. Suppose Assumption 2 holds. Then the expected 1-Wasserstein distance between the ecdf of the observed belief distribution  $\hat{F}_n$  and the cdf of the initial belief distribution  $F$  has the*

following upper bound,

$$\begin{aligned} \mathbb{E} \left[ W_1(\hat{F}_n, F) \right] &\leq \frac{1}{n} \int_{\mathbb{R}} \sqrt{\sum_{i=1}^n \tilde{F}_{d_i^o+1}(t)(1 - \tilde{F}_{d_i^o+1}(t))} dt \\ &+ \sigma \sqrt{2(1 - \rho^{F, \tilde{F}})} + \sigma \left( 1 - \frac{1}{n} \sum_{i=1}^n \frac{1}{\sqrt{d_i^o + 1}} \right) + \frac{\sigma}{n} \sum_{i=1}^n \sqrt{\frac{2(1 - \rho^{F^{d_i^o+1}, \tilde{F}^{d_i^o+1}})}{d_i^o + 1}} \\ &+ \frac{O(\langle d^o \rangle)}{\sqrt{n}} \end{aligned}$$

where  $\rho^{F, \tilde{F}}$  and  $\rho^{F^{d_i^o+1}, \tilde{F}^{d_i^o+1}}$  are the respective Pearson correlation of the points in the quantile-quantile plot of  $F$  and  $\tilde{F}$ , and  $F^{d_i^o+1}$  and  $\tilde{F}^{d_i^o+1}$  for  $i \in [n]$  and  $\langle d^o \rangle$  is the average degree of  $\tilde{G}^d$ .

Although the main difference in the derivation of Corollary 2 and Proposition 3 lies in the directionality of the network, we are still able to distinguish the two main effects: the interaction and sample size effects in the respective terms of Corollary 2 from similar terms. As the bounds depend on the out-degree of every respondent, policymakers need to pay more attention to “highly-influential” respondents (i.e., those with high out-degree) due to their stronger ability to shape policy beliefs. On the other hand, respondents with low out-degree contribute less to the interaction effect.

As mentioned in Subsection 4.4, the population network affects the resulting subgraph through the sampling process. Hence, in the spirit of the problem context, we need to consider the population network instead of a fixed subgraph. In this case, using the law of iterated expectation, we have an analogous representation of the expected 1-Wasserstein distance between the ecdf of the observed belief distribution and the cdf of the initial belief distribution in the directed network setting, which is similar to that of Corollary 1. We provide the following corollary and its expansion is similar to that given in Appendix B.

**Corollary 3.** *Given the directed population graph  $G^d(P, E^d)$ , the expected 1-Wasserstein distance between the ecdf  $\hat{F}_n$  and the cdf of the initial belief distribution  $F$  is given as*

$$\mathbb{E}[W_1(\hat{F}_n, F)] = \mathbb{E} \left[ \mathbb{E} \left[ W_1(\hat{F}_n, F) | \tilde{G}^d \right] \right]$$

where the inner expectation is from Corollary 2, which we then take the expectation over all possible resulting directed subgraphs that consist of  $n$  respondents.

### 5.3 General Interaction Rules

Our analysis thus far assumed that every respondent listens to each of their neighbor to the same extent and updates one’s belief by taking a simple average. However, respondents can have a preference for who they would listen to and update their beliefs differently. To model this, we allow the respondents to place different weights on his/her own and their neighbors’ beliefs. As such, the sampled respondents follow the weighted average interaction rule.

Suppose that the policymakers adopt the random sampling strategy and sample  $n$  respondents from the population uniformly at random. Let the initial beliefs of each of the respondents be a random variable as denoted by  $X_1, X_2, \dots, X_n$ , which are drawn i.i.d. from  $\mathcal{F}^*$ . We denote the random variable of the updated belief of each sampled respondent  $i$  to be  $X_i^a := \sum_{j \in N_i^d \cup i} a_{ij} X_j$ , where  $a_{ij}$  is the normalized tendency for respondent  $i$  to listen to respondent  $j$  after they interact. Then, the ecdf of the observed belief distribution,  $\hat{F}_n(t)$  is given as

$$\hat{F}_n(t) = \frac{1}{n} \sum_{i=1}^n \mathbb{1}(X_i^a \leq t)$$

Let the random variable  $X_i^a$  follows a weighted sample mean distribution. We denote the resulting distribution  $\mathcal{C}_i$ , and we denote the corresponding cdf as  $C_i$ , for all  $i \in \{1, 2, \dots, n\}$ . Then, the mean and standard deviation of  $\mathcal{C}_i$  is  $\mu$  and  $\sigma \sqrt{\sum_{j \in N_i^d \cup i} a_{ij}^2}$  respectively. We let  $Y_i^a(t)$  be the indicator variable  $\mathbb{1}(X_i^a \leq t)$ . For a fixed  $t$ , the indicator variable  $Y_i^a(t)$  is a Bernoulli random variable, where

$$Y_i^a(t) = \begin{cases} 1 & \text{w.p. } C_i(t) \\ 0 & \text{w.p. } 1 - C_i(t) \end{cases}$$

Then,  $\mathbb{E}[Y_i^a(t)] = C_i(t)$  and  $\text{Var}(Y_i^a(t)) = C_i(t)(1 - C_i(t))$ . We note that the analysis of the expected 1-Wasserstein distance for a general interaction rule is analogous to the analysis in Subsection 4.4, where we have to account for the number of common edges and neighbors. Hence, we apply the results from Claim 1 and Assumption 1 into our following analysis. Using similar proof techniques from Proposition 3, we now have the following corollary with  $\tilde{F}$  and  $\tilde{F}_i$  to be the cdfs of the normal distributions  $N(\mu, \sigma^2)$  and  $N(\mu, \sigma^2 \sum_{j \in N_i^d \cup i} a_{ij}^2)$  for  $i \in [n]$ .

**Corollary 4.** *Given the resulting subgraph  $\tilde{G}$  obtained by randomly selecting  $n$  respondents. Suppose Assumption 1 holds. Then the expected 1-Wasserstein distance between the ecdf of the observed belief distribution  $\hat{F}_n$  and the cdf of the initial belief distribution  $F$  has the following upper bound,*

$$\begin{aligned} \mathbb{E} \left[ W_1(\hat{F}_n, F) \right] &\leq \frac{1}{n} \int_{\mathbb{R}} \sqrt{\sum_{i=1}^n C_i(t)(1 - C_i(t))} dt \\ &\quad + \sigma \sqrt{2(1 - \rho^{F, \tilde{F}})} + \sigma + \frac{\sigma}{n} \sum_{i=1}^n \sqrt{\sum_{j \in N_i^d \cup i} a_{ij}^2} \left( \sqrt{2(1 - \rho^{C_i, \tilde{F}_i})} - 1 \right) \\ &\quad + \frac{O(\langle d \rangle)}{\sqrt{n}} \end{aligned}$$

where  $\rho^{F, \tilde{F}}$  and  $\rho^{C_i, \tilde{F}_i}$  are the respective Pearson correlation of the points in the quantile-quantile plot of  $F$  and  $\tilde{F}$ , and  $C_i$  and  $\tilde{F}_i$  for  $i \in [n]$  and  $\langle d \rangle$  is the average degree of  $\tilde{G}$ .

Although the main difference in the derivation of Corollary 4 and Proposition 3 lies in the degree of interaction among the respondents, we are still able to distinguish the two main effects: the interaction and sample size effects in the respective terms of Corollary 2 from similar terms. Despite these personalized weights  $a_{ij}$  reflecting a more nuanced dynamic, policymakers may need to carry out more sophisticated studies to obtain these values. Similar to the analysis in



the earlier subsection, we need to consider the general population network. Hence, we provide the following corollary and its expansion resembles that in Appendix B.

**Corollary 5.** *For a given population graph  $G(P, E)$ , the expected 1-Wasserstein distance between the ecdf  $\hat{F}_n$  and the cdf of the initial belief distribution  $F$  is given as*

$$\mathbb{E}[W_1(\hat{F}_n, F)] = \mathbb{E} \left[ \mathbb{E} \left[ W_1(\hat{F}_n, F) | \tilde{G} \right] \right]$$

where the inner expectation is from Corollary 4, which we then take the expectation over all possible resulting subgraphs that consist of  $n$  respondents.

## 6 Numerical experiments

In this section, we conduct several numerical experiments to compute and analyze the 1-Wasserstein distances for different sampling strategies across various underlying graphical structures and degrees of interaction. To generate the population network, we employ two common random graph-based models, specifically the Erdős-Renyi (E-R) (Erdős & Rényi, 1960) and the scale-free (S-F) networks (Goh et al., 2001). Apart from these models, we use two large-scale network datasets from the Stanford Network Analysis Platform (SNAP) (Leskovec & Krevl, 2014) for our numerical analyses. As the support of the policy belief distribution could be either bounded or unbounded, we consider two notable probability distributions, specifically the beta and the standard normal distributions, with varying parameters. We employ the same three sampling strategies discussed in the earlier theoretical analysis. For the independent set sampling strategy, we generate a maximal independent set from a given population network using Algorithm 1. For the random sample, we randomly select half of the population. For the cluster sampling strategy, we first detect the clusters using a greedy modularity optimization algorithm (Clauset et al., 2004), one that has been used in recent studies (Nadini et al., 2021; Hernandez et al., 2021). We then randomly select half the number of clusters and expose every respondent in the selected clusters to the policy.

By setting the total population to 500, we conduct a series of numerical experiments with different parameters as listed in the following table. We examine various characteristics of the initial belief distribution, such as asymmetric distribution shape and unbounded support. The asymmetrical shape mimics the situation where the population has relatively strong or weak support for the policy, while the unbounded support allows the belief values to take up any real number. We also consider different interaction rules to mimic different degrees of influence that neighbors have on a respondent. To construct the stochastic matrix that models the weighted average rule, we generate a random matrix, where each entry is drawn from a uniform distribution over  $[0, 1)$ , which we then normalize every entry across each row. We generate an empirical distribution of the 1-Wasserstein distance between the initial and updated belief distributions across multiple settings by running the numerical experiments 500 times. We show the empirical distributions as a boxplot in the respective figures.

Boxplots	Initial belief distribution	Interaction Rule
Figures 1, 7a, 8a, 9a	Beta(2,2)	average interaction rule
Figures 2, 7b, 8b, 9b	Beta(2,2)	weighted interaction rule
Figures 3, 7c, 8c, 9c	Beta(2,5)	average interaction rule
Figures 4, 7d, 8d, 9d	Beta(2,5)	weighted interaction rule
Figures 5, 7e, 8e, 9e	Normal(0,1)	average interaction rule
Figures 6, 7f, 8f, 9f	Normal(0,1)	weighted interaction rule

Table 1: Different parameters on initial belief distribution and interaction mechanism over various graphs

After setting up the parameters of the numerical experiment, we first consider the E-R model. Asymptotically, there is a phase transition in the E-R graph changes once the probability  $p(|V|)$ , where the population size  $|V|$ , exceeds a certain threshold (Jackson et al., 2008). For example, edges start to emerge at the threshold of  $p(|V|) = \frac{1}{|V|^2}$  in the limit. Hence, we conduct the numerical experiments across different edge probabilities, specifically,  $\frac{1}{|V|^2}$ ,  $\frac{1}{|V|^{1.5}}$ ,  $\frac{1}{|V|}$ ,  $\frac{1}{|V|^{0.5}}$ ,  $\frac{1}{|V|^{0.25}}$ ,  $\frac{1}{|V|^{0.125}}$ , where  $|V|=500$ . We provide the boxplots of the 1-Wasserstein distance for each of the six probabilities in the following figures, as well as several statistical results such as the mean distance and the Kolmogorov-Smirnov (K-S) test statistics in Appendix C.

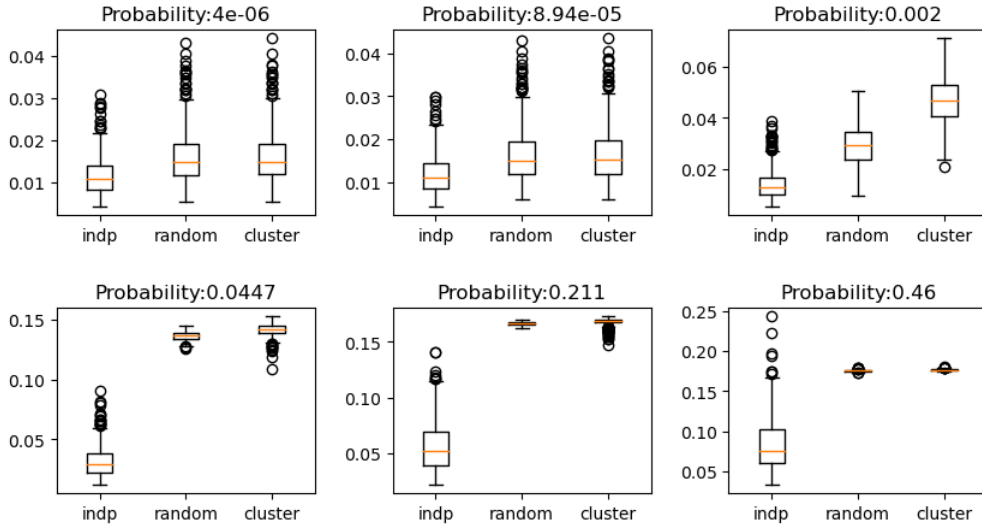


Figure 1: Initial belief distribution: Beta(2,2), Average interaction rule

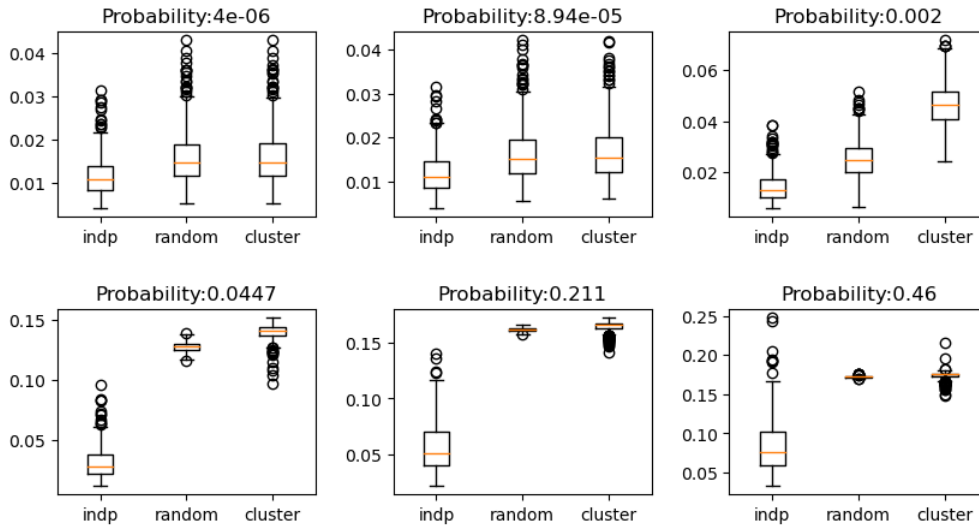


Figure 2: Initial belief distribution: Beta(2,2), Weighted interaction rule

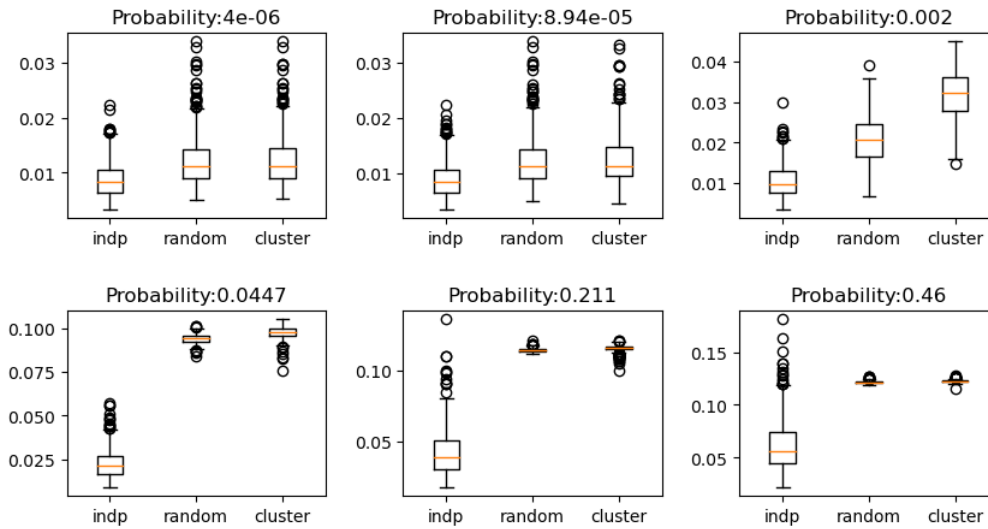


Figure 3: Initial belief distribution: Beta(2,5), Average interaction rule

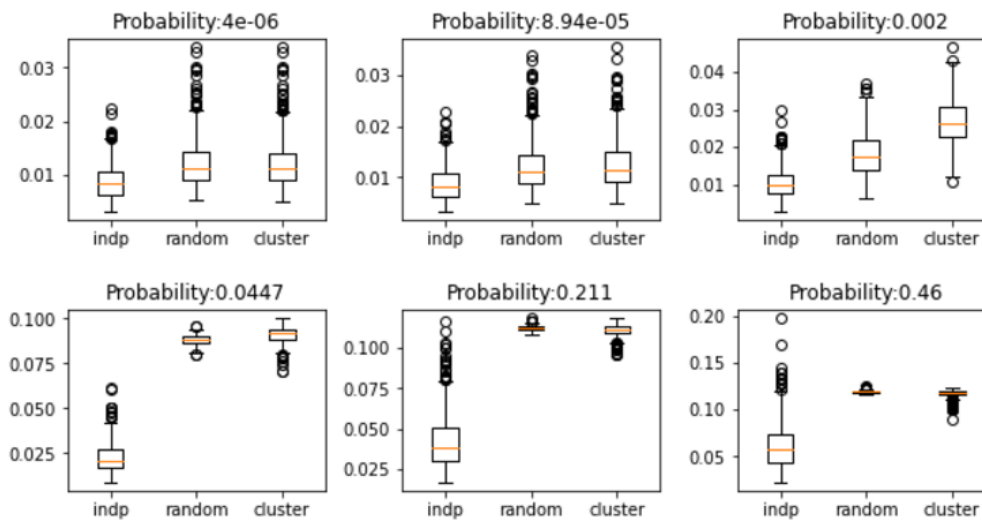


Figure 4: Initial belief distribution: Beta(2,5), Weighted interaction rule

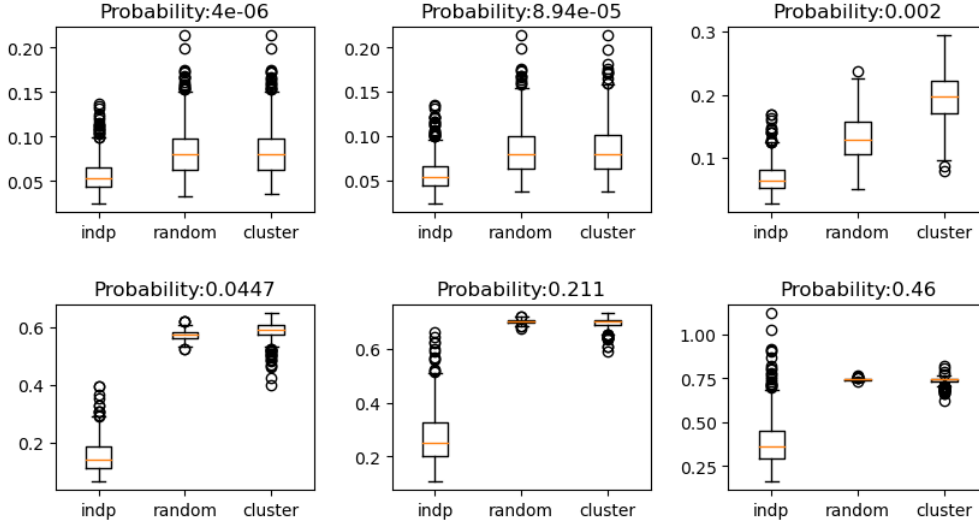


Figure 5: Initial belief distribution: Normal(0,1), Average interaction rule

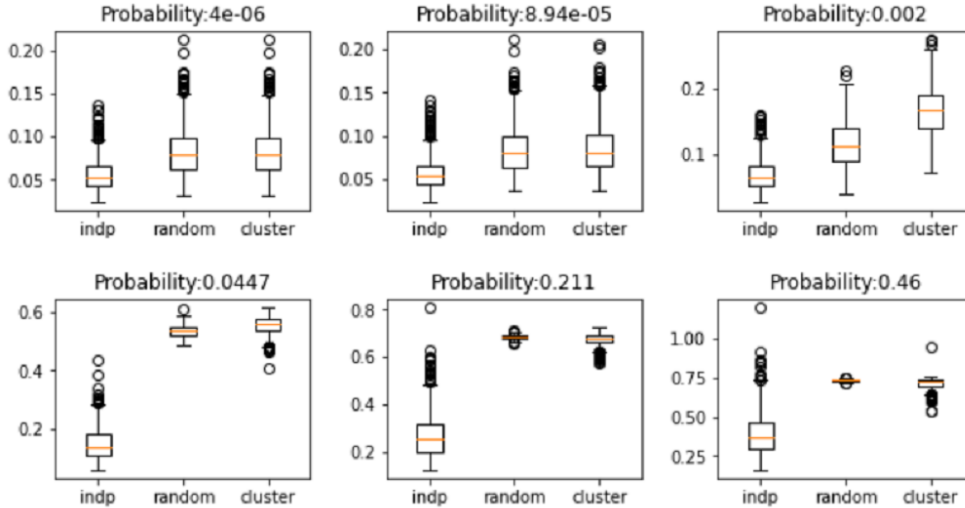


Figure 6: Initial belief distribution: Normal(0,1), Weighted interaction rule

We observe that at small edge probabilities, all three sampling strategies have a small mean 1-Wasserstein distance and the boxplots have a long tail. Since the edge probabilities are small, the resulting subgraphs after sampling have few edges. Then, the random and cluster samples largely consist of isolated vertices and there would be minimal interaction effect. Hence, the random and cluster samples perform almost as well as an independent set sample and all three sampling strategies could accurately estimate the initial belief distribution with small error. As the edge probability increases, the size of the independent set sample decreases, which thus affects the estimation of the initial belief distribution, as reflected in the increase of the 1-Wasserstein distance. There is also an increase in the 1-Wasserstein distance for the random and cluster samples due to a larger interaction effect arising from a larger edge probability and more edges in the resulting subgraph. We note that there is a larger shift in the boxplots for the random and cluster samples as compared to that of the independent set sample. This suggests that the increased interaction effect in the sample affects the estimation of the initial belief

distribution through the 1-Wasserstein distance more strongly than the reduction in the size of the independent set sample.

We note that the variance of the empirical 1-Wasserstein distance distribution of the random and cluster samples decreases as the edge probability increases. As respondents have more neighbors, most tend to reach a consensus and share similar beliefs after interacting, thus contributing to similar empirical 1-Wasserstein distance distributions across the runs. Interestingly, the estimation performance of the random and cluster samples at a smaller probability is similar to that of the independent set sample at a larger probability. Hence, if the population network is extremely sparse and there is minimal interaction effect, a random sampling strategy would be preferred as policymakers need a substantial independent set size to achieve a similar estimation performance, which could be difficult to obtain due to resources and feasibility constraints.

We also notice that by introducing asymmetry in the belief distribution, while keeping the other parameters unchanged, there is a smaller mean 1-Wasserstein distance as compared to the symmetrical counterparts across all threshold probabilities (see Tables 2 to 7 in Appendix C). We postulate that in an asymmetrical distribution, most beliefs are concentrated within a smaller interval due to the initial belief distribution shape and are unlikely to deviate too much after interacting. Thus, there would be a smaller difference between the updated and the initial belief distributions.

Next, we investigate different degrees of interaction among the respondents. We observe that with a moderately large edge probability, the mean 1-Wasserstein distance for the random and cluster sampling strategies are slightly larger than those of the weighted counterparts (see Tables 2 to 7 in Appendix C). Furthermore, the differences in the empirical 1-Wasserstein distance distributions are significant at 5% level of significance (see Tables 8 to 10 in Appendix C). A plausible reason for the significant difference in the empirical distribution is the network density. We postulate that as the network density increases, respondents tend to have more neighbors (i.e., a larger degree). Then, the normalized influence that an influential neighbor has on a respondent “dilutes” and the magnitude of influence would be similar to that of the other neighbors on the same respondent.

We also observe a larger mean 1-Wasserstein distance across all sampling strategies and probabilities thresholds for the unbounded belief distribution support as compared to the bounded counterparts (see Tables 2 to 7 in Appendix C). Since we are accounting for the difference in the density functions over a larger support, this could lead to a greater 1-Wasserstein distance.

Next, we consider another random graph-based model, the S-F model, where the generated networks have a scale-free property, i.e., the graph has a power law degree distribution. We consider a scale factor of 2.5 as many scale-free networks have scaling exponents between 2 and 3 (Goh et al., 2002; Chen & Shi, 2004; Goh et al., 2001; Barabási, 2016). We set the network size for the S-F models to 998, which is close to the expected size of the E-R graph with edge

probability  $\frac{1}{|V|}$ , where  $|V|=500$ .

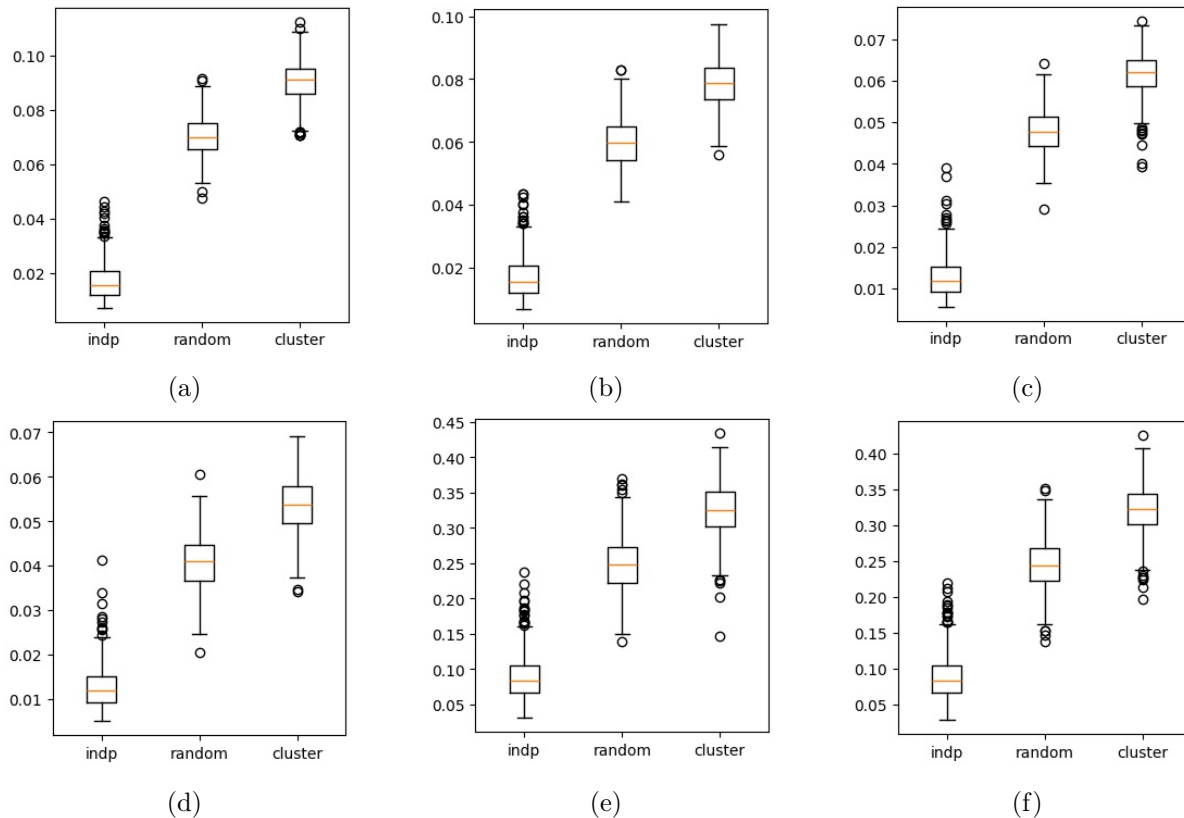


Figure 7: S-F model

As graphs generated by the S-F model have a power law degree distribution, most vertices have few degrees and policymakers can obtain a sizeable independent set sample. As evident from all the subfigures, the independent set sampling strategy generates the smallest mean 1-Wasserstein distance. In addition, the random sample would consist of a mixture of isolated vertices and small components due to the power law degree distribution, thus the mean 1-Wasserstein distance for the random sampling strategy is larger than that of the independent set strategy and smaller than that of the cluster sampling strategy.

Apart from using a random graph-based method to generate the underlying network, we use several real-life datasets for our numerical experiments. We use the `ego-Facebook` dataset from SNAP (Leskovec & Krevl, 2014), which consists of friends lists from Facebook. There are 4039 vertices and 88234 edges and we observe that this network has *small-world* properties as it has a moderately high average clustering coefficient of 0.6055 and a small average path length of 3.69. We also mimic the situation where policymakers do not have much resources and can only access a small independent set sample. In this case, we study two scenarios where the size of the independent set sample is 10 and 30 respectively.

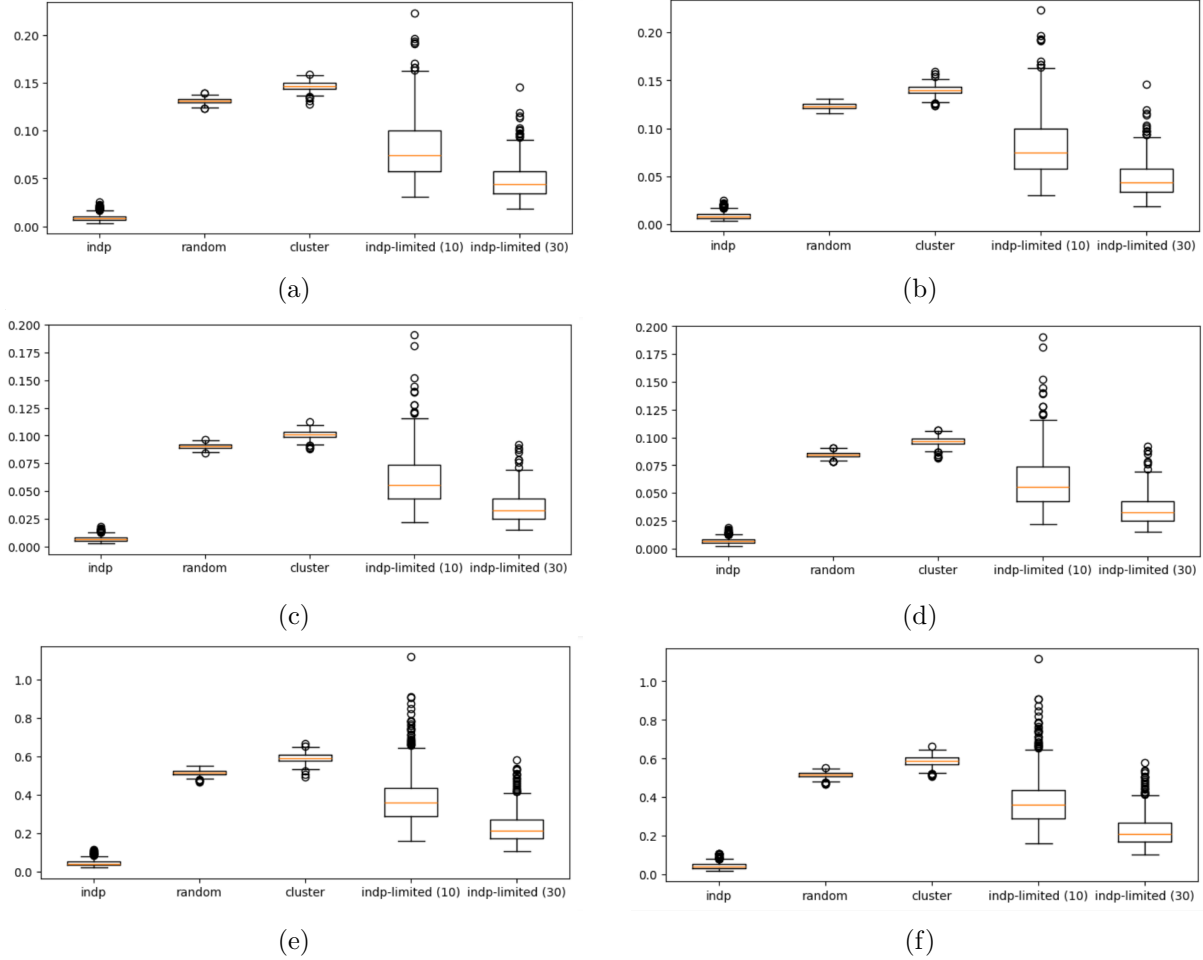


Figure 8: Using `ego-Facebook` dataset from SNAP

As evident in the subfigures in Figure 8, the mean 1-Wasserstein distance for the independent set sampling strategy is much smaller than that of the random and cluster sampling strategies. As real-world networks are relatively sparse, we could obtain a large independent set sample, allowing for an accurate estimation of the initial belief distribution. Even with a small independent set sample, we also obtain a smaller mean 1-Wasserstein distance than those by the random and cluster samples. However, there is a larger variance due to the small sample size. We also observe that a sizeable independent sample set helps distinguish and differentiate the empirical distribution attributed to the sample size effect induced by the independent set sampling strategy and the interaction effect induced by the random and cluster sampling strategies.

Lastly, we use the directed `email-Eu-core` network dataset from SNAP (Leskovec & Krevl, 2014) to incorporate network directionality into our numerical analyses. This network dataset was generated using email data from a large European research institution, with 81306 vertices and 1768149 edges in this directed network. Some descriptive statistics include an average clustering coefficient of 0.3994 and an average path length of 2.544 in the giant component. Similar to the previous numerical experiment, we include the case where we have a small independent set sample of sizes 10 and 30.

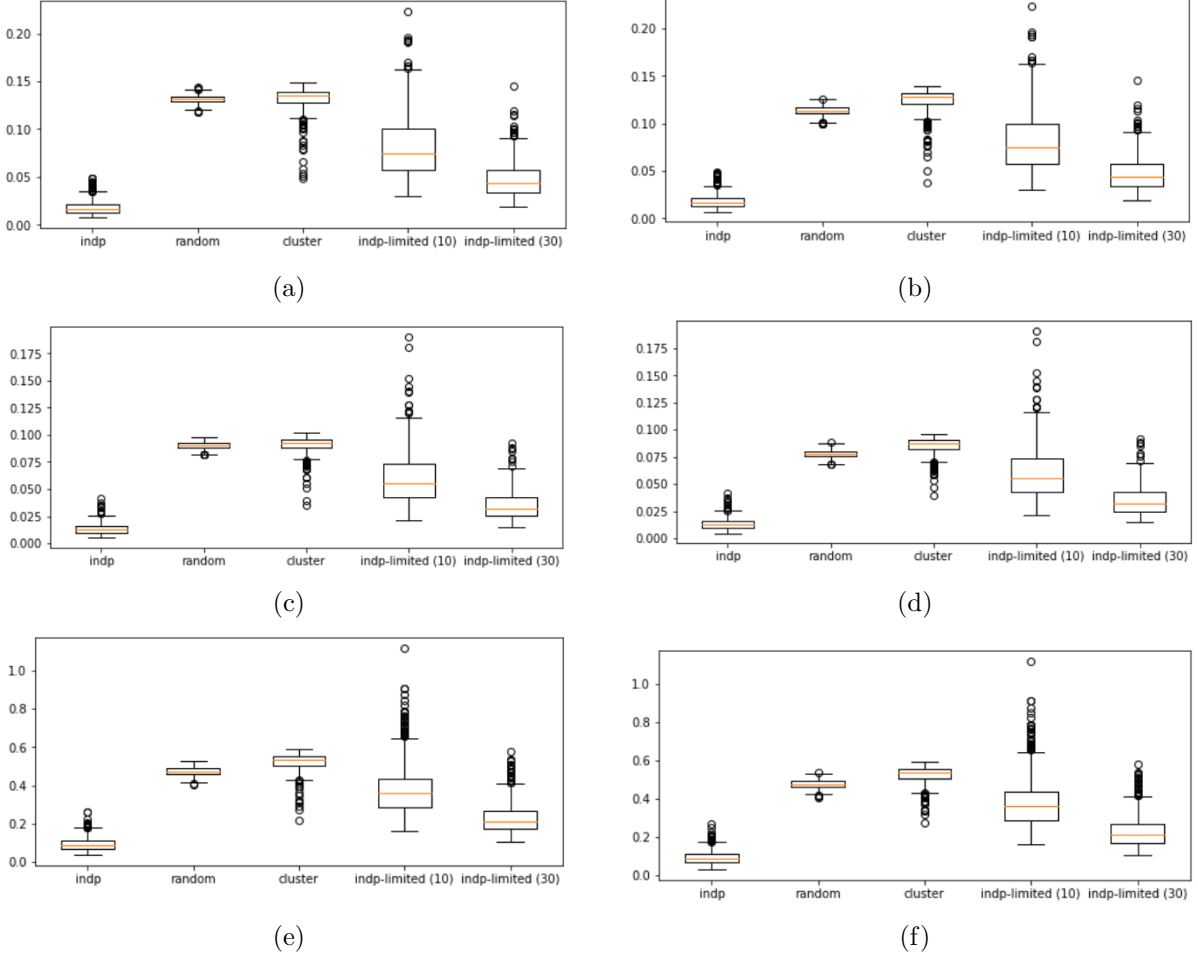


Figure 9: Using `ego-Eu-core` dataset from SNAP

We observe a similar shape in the empirical 1-Wasserstein distance distribution between corresponding subfigures in Figures 8 and 9. As the density in both real-world networks is close to the reciprocal of the number of vertices, we notice a similar distribution shape as compared to the respective subfigures in Figures 1 to 6 with edge probability  $\frac{1}{|V|}$ . We also consider an undirected version of the `email-Eu-core` network dataset. By comparing the empirical 1-Wasserstein distance distributions using the 2-sample K-S test between the directed and undirected versions under the same initial belief distribution and interaction rule, we investigate how directionality in the network affects the distance. We compute and list their mean 1-Wasserstein distances, the Kolmogorov-D statistic and their  $p$ -values in Tables 11, 12 and 13 in Appendix C. We observe that the mean 1-Wasserstein distances for the directed version are generally slightly larger than the undirected counterparts, where the differences are significant at the 1% significance level. This implies that directionality in the network is not a critical factor in affecting the estimation of the initial belief distribution.

## 7 Conclusion and Future Directions

In our work, we attempt to estimate the initial policy responses and quantify the deviation from an empirically observed belief distribution using the Wasserstein metric. As several factors af-



fect the empirical data, such as the sampling strategies, the underlying network topology and how the respondents interact, we investigate how each factor influences the Wasserstein distance analytically. We mainly consider three different sampling strategies, namely independent set sampling, random sampling and cluster sampling, to model how respondents are selected for the policy evaluation studies. Under a stipulated interaction mechanism, we theoretically provide an upper bound to the expected 1-Wasserstein distance between the initial and empirically observed belief distributions. As there is a size limit to the independent set sample and potential interactions induced by the other two strategies, we study the tradeoff between these two effects: sample size and interaction effects. We also consider other graphical structures such as directed networks and a generalized interaction mechanism to mimic certain real-life phenomena such as dissimilar tendencies of belief adoption. Lastly, we conduct several numerical analyses based on generated networks and real-life network datasets to illustrate how the three different factors affect the estimation of the initial policy responses and the deviation quantified by the 1-Wasserstein distance.

In this current study, we design interaction mechanisms and sampling strategies to model how policy evaluation studies are carried out in real life. Our work aims to provide a conceptual framework for policymakers to estimate the initial policy responses and quantify the deviation from the observed data, which has clear practical implications in evaluating policy effectiveness. However, we need to discuss some of our assumptions and the limitations of our model. First, our model does not consider the natural tendency of respondents to change their own beliefs and incorporate external factors that could potentially shape their perspectives. Although a controlled and closed setting may be a strict assumption under various contexts, this stylized environment allows policymakers to recognize and quantify the tradeoff between the two effects. Second, our work only considers static networks to simplify the estimation of initial belief distribution. We acknowledge that beliefs can change over time due to various reasons, hence, another avenue for future research is to incorporate dynamic network processes such as changing levels of interaction over time or homophily where respondents form new edges due to similar policy responses. This, in turn, influences the spread of information and attitudes within social networks. Despite the heightened difficulty, policymakers can attempt to develop a mechanism to incorporate temporal dynamics into the statistical inference. Lastly, we note the difficulty of estimating the exact shape and moments of the initial belief distribution under limited data and unspecified network dynamics. An interesting future direction is to provide such structural characteristics of the belief distribution to understand the nuances in the beliefs and behaviors of the population better.

## Acknowledgments

The authors would like to thank Dr. Prasanta Bhattacharya for his comments on the manuscript.

## References

- Abrams, D., & Levine, J. (2012). The formation of social norms: Revisiting sherif’s autokinetic illusion study. *Social Psychology: Revisiting the Classic Studies*, 57–75.
- Allen, J., Watts, D. J., & Rand, D. G. (2024). Quantifying the impact of misinformation and vaccine-skeptical content on facebook. *Science*, 384(6699), eadk3451.
- Ang, E. T., Bhattacharya, P., & Lim, A. E. (2025). Estimating policy effects in a social network with independent set sampling. *Social Networks*, 81, 17–30.
- Aronow, P. M. (2012). A general method for detecting interference between units in randomized experiments. *Sociological Methods & Research*, 41(1), 3–16.
- Aronow, P. M., & Samii, C. (2017). Estimating average causal effects under general interference, with application to a social network experiment.
- Athey, S., & Imbens, G. W. (2017). The state of applied econometrics: Causality and policy evaluation. *Journal of Economic Perspectives*, 31(2), 3–32.
- Barabási, A. (2016). *Network science*. Cambridge University Press.
- Blelloch, G. E., Fineman, J. T., & Shun, J. (2012). Greedy sequential maximal independent set and matching are parallel on average. *Proceedings of the twenty-fourth annual ACM symposium on Parallelism in algorithms and architectures*, 308–317.
- Bowers, J., Fredrickson, M. M., & Panagopoulos, C. (2013). Reasoning about interference between units: A general framework. *Political Analysis*, 21(1), 97–124.
- Burstein, P. (2003). The impact of public opinion on public policy: A review and an agenda. *Political research quarterly*, 56(1), 29–40.
- Cai, J., De Janvry, A., & Sadoulet, E. (2015). Social networks and the decision to insure. *American Economic Journal: Applied Economics*, 7(2), 81–108.
- Cai, Y., & Lim, L.-H. (2022). Distances between probability distributions of different dimensions. *IEEE Transactions on Information Theory*, 68(6), 4020–4031.
- Castellano, C., Fortunato, S., & Loreto, V. (2009). Statistical physics of social dynamics. *Reviews of modern physics*, 81(2), 591.
- Chen, Q., & Shi, D. (2004). The modeling of scale-free networks. *Physica A: Statistical Mechanics and its Applications*, 335(1-2), 240–248.
- Clauset, A., Newman, M. E., & Moore, C. (2004). Finding community structure in very large networks. *Physical review E*, 70(6), 066111.
- Deffuant, G., Neau, D., Amblard, F., & Weisbuch, G. (2000). Mixing beliefs among interacting agents. *Advances in Complex Systems*, 3(01n04), 87–98.
- DeGroot, M. H. (1974). Reaching a consensus. *Journal of the American Statistical association*, 69(345), 118–121.
- Eckles, D., Karrer, B., & Ugander, J. (2017). Design and analysis of experiments in networks: Reducing bias from interference. *Journal of Causal Inference*, 5(1), 20150021.
- Erdős, P., & Rényi, A. (1960). On the evolution of random graphs. *Publ. math. inst. hung. acad. sci*, 5(1), 17–60.
- Fatemi, Z., & Zheleva, E. (2023). Network experiment designs for inferring causal effects under interference. *Frontiers in big Data*, 6, 1128649.

- Forastiere, L., Airoidi, E. M., & Mealli, F. (2021). Identification and estimation of treatment and interference effects in observational studies on networks. *Journal of the American Statistical Association*, *116*(534), 901–918.
- Frogner, C., Zhang, C., Mobahi, H., Araya, M., & Poggio, T. A. (2015). Learning with a wasserstein loss. *Advances in neural information processing systems*, *28*.
- Gini, C. (1914). Di una misura di dissomiglianza tra due gruppi di quantitae delle sue applicazioni allo studio delle relazioni statistiche. *Atti del R. Istituto Veneto di Scienze Lettere e Arti LXXIII*.
- Goh, K.-I., Kahng, B., & Kim, D. (2001). Universal behavior of load distribution in scale-free networks. *Physical review letters*, *87*(27), 278701.
- Goh, K.-I., Oh, E., Jeong, H., Kahng, B., & Kim, D. (2002). Classification of scale-free networks. *Proceedings of the National Academy of Sciences*, *99*(20), 12583–12588.
- Goldstein, C. E., Weijer, C., Brehaut, J. C., Fergusson, D. A., Grimshaw, J. M., Horn, A. R., & Taljaard, M. (2018). Ethical issues in pragmatic randomized controlled trials: A review of the recent literature identifies gaps in ethical argumentation. *BMC medical ethics*, *19*, 1–10.
- Golub, B., & Jackson, M. O. (2010). Naive learning in social networks and the wisdom of crowds. *American Economic Journal: Microeconomics*, *2*(1), 112–149.
- González-Bailón, S. (2013). Social science in the era of big data. *Policy & internet*, *5*(2), 147–160.
- Grelle, S., & Hofmann, W. (2024). When and why do people accept public-policy interventions? an integrative public-policy-acceptance framework. *Perspectives on Psychological Science*, *19*(1), 258–279.
- Hariton, E., & Locascio, J. (2018). Randomised controlled trials - the gold standard for effectiveness research: Study design: Randomised controlled trials. *BJOG: An International Journal of Obstetrics & Gynaecology*, *125*(13), 1716.
- Hegselmann, R., Krause, U., et al. (2002). Opinion dynamics and bounded confidence models, analysis, and simulation. *Journal of artificial societies and social simulation*, *5*(3).
- Hernandez, D. J., David, A. S., Menges, E. S., Searcy, C. A., & Afkhami, M. E. (2021). Environmental stress destabilizes microbial networks. *The ISME journal*, *15*(6), 1722–1734.
- Holley, R. A., & Liggett, T. M. (1975). Ergodic theorems for weakly interacting infinite systems and the voter model. *The annals of probability*, 643–663.
- Irpino, A., & Verde, R. (2015). Basic statistics for distributional symbolic variables: A new metric-based approach. *Advances in Data Analysis and Classification*, *9*, 143–175.
- Jackson, M. O., et al. (2008). *Social and economic networks* (Vol. 3). Princeton university press Princeton.
- Jones, M. D., & Jenkins-Smith, H. C. (2009). Trans-subsystem dynamics: Policy topography, mass opinion, and policy change. *Policy studies journal*, *37*(1), 37–58.
- Karwa, V., & Airoidi, E. (2018). A systematic investigation of classical causal inference strategies under mis-specification due to network interference. *arXiv preprint arXiv:1810.08259*.
- Kline, B., & Tamer, E. (2014). Some interpretation of the linear-in-means model of social interactions.

- Larsen, K. S. (1990). The asch conformity experiment: Replication and transhistorical comparison. *Journal of Social Behavior and Personality*, 5(4), 163.
- Leo, J., Ge, E., & Li, S. (2023). Wasserstein distance in deep learning. *Available at SSRN 4368733*.
- Leskovec, J., & Krevl, A. (2014). SNAP Datasets: Stanford large network dataset collection.
- Leung, M. P. (2020). Treatment and spillover effects under network interference. *Review of Economics and Statistics*, 102(2), 368–380.
- Lorenz, J. (2007). Continuous opinion dynamics under bounded confidence: A survey. *International Journal of Modern Physics C*, 18(12), 1819–1838.
- Manski, C. F. (1993). Identification of endogenous social effects: The reflection problem. *The Review of Economic Studies*, 60(3), 531–542.
- Nadini, M., Alessandretti, L., Di Giacinto, F., Martino, M., Aiello, L. M., & Baronchelli, A. (2021). Mapping the nft revolution: Market trends, trade networks, and visual features. *Scientific reports*, 11(1), 20902.
- OECD. (2020). *Improving governance with policy evaluation*.
- Peralta, A. F., Kertész, J., & Iñiguez, G. (2022). Opinion dynamics in social networks: From models to data. *arXiv preprint arXiv:2201.01322*.
- Persson, M. (2021). From opinions to policies: Examining the links between citizens, representatives, and policy change. *Electoral Studies*, 74, 102413.
- Rachev, S. T., & Rüschendorf, L. (1998). *Mass transportation problems: Volume i: Theory* (Vol. 1). Springer Science & Business Media.
- Redner, S. (2019). Reality-inspired voter models: A mini-review. *Comptes Rendus Physique*, 20(4), 275–292.
- Sherif, M. (1937). An experimental approach to the study of attitudes. *Sociometry*, 1(1/2), 90–98.
- Sobkowicz, P. (2009). Modelling opinion formation with physics tools: Call for closer link with reality. *Journal of Artificial Societies and Social Simulation*, 12(1), 11.
- Tchetgen, E. J. T., & VanderWeele, T. J. (2012). On causal inference in the presence of interference. *Statistical methods in medical research*, 21(1), 55–75.
- Ugander, J., Karrer, B., Backstrom, L., & Kleinberg, J. (2013). Graph cluster randomization: Network exposure to multiple universes. *Proceedings of the 19th ACM SIGKDD international conference on Knowledge discovery and data mining*, 329–337.
- Ugander, J., & Yin, H. (2023). Randomized graph cluster randomization. *Journal of Causal Inference*, 11(1), 20220014.
- Van Crombrugge, R. (2021). Are referendums necessarily populist? countering the populist interpretation of referendums through institutional design. *Representation*, 57(1), 109–130.
- Villani, C., et al. (2009). *Optimal transport: Old and new* (Vol. 338). Springer.
- Wagenaar, C. C. (2019). *Referendums can be more effective if voters can choose from several options*. <https://www.democraticaudit.com/2019/11/01/referendums-can-be-more-effective-if-voters-can-choose-from-several-options/>
- West, D. (1996). *Introduction to graph theory*. Prentice Hall.

Xia, H., Wang, H., & Xuan, Z. (2011). Opinion dynamics: A multidisciplinary review and perspective on future research. *International Journal of Knowledge and Systems Science (IJKSS)*, 2(4), 72–91.

## Appendix A Algorithm for Sampling Independent Sets

In this section, we present a pseudocode that we employ to obtain our independent set samples. We adopt an iterative approach to obtain the independent set for our numerical studies, as used in other studies (Blelloch et al., 2012). We provide the following definition to complement our algorithm.

**Definition 2.** A graph  $G'(V', E')$  is a subgraph of  $G(V, E)$  where  $V' \subseteq V$  and  $E' \subseteq E$ . For a subset of nodes  $V' \subseteq V$ , the subgraph of  $G$  induced by  $V'$  is the subgraph  $G'(V', E')$ , where  $E' = E \cap \binom{V'}{2}$ . A vertex-induced subgraph contains a subset of vertices, coupled with edges whose endpoints are both in the subset.

We also add a size limit parameter into the pseudocode to provide flexibility in controlling the size of the independent set. In our numerical studies, we do not limit ourselves to a specific independent set size, so we set  $S = |V(G)|$ .

---

### Algorithm 1 Iterative Independent Set Selection

---

**Input:** Graph  $G$ , Size  $S$

**Output:** Independent Set  $I$

```

1: while  $G \neq \emptyset$  do
2:   Randomly select a vertex  $v \in V(G)$ 
3:    $I \leftarrow I \cup v$ 
4:    $G \leftarrow \tilde{G}$ , where  $\tilde{G}$  is the vertex-induced subgraph of  $V(G) \setminus (v \cup N_v)$ 
5:   if  $|I| > S$  then
6:     break
7:   end if
8: end while
9: return  $I$ 

```

---

## Appendix B Expansion of Corollary 1

We recall that there are two independent elements of randomness in the problem context, the sampling strategy and the initial beliefs of the respondents. We first fix the sampled respondents, thus determining the resulting subgraph  $\tilde{G}$ . Then, by the law of iterated expectation, we have

$$\mathbb{E} \left[ W_1(\hat{F}_n, F) \right] = \mathbb{E} \left[ \mathbb{E} \left[ W_1(\hat{F}_n, F) | \tilde{G} \right] \right]$$

From Proposition 3, we have the upper bound of  $\mathbb{E} \left[ W_1(\hat{F}_n, F) | \tilde{G} \right]$ . As the degree of the selected respondents changes across various resulting subgraphs, we need to take the expectation over all possible selection of  $n$  respondents. By Fubini's theorem and Jensen's inequality, the first

and third rows in the upper bound of Proposition 3 are given as,

$$\begin{aligned} & \mathbb{E} \left[ \frac{1}{n} \int_{\mathbb{R}} \sqrt{\sum_{i=1}^n F^{d_i+1}(t)(1 - F^{d_i+1}(t)) + \frac{\sum_{r \neq s}^n M_{r,s}}{4}} dt \right] \\ & \leq \frac{1}{n} \int_{\mathbb{R}} \sqrt{\mathbb{E} [\sum_{i=1}^n F^{d_i+1}(t)(1 - F^{d_i+1}(t))] + \frac{\mathbb{E} [\sum_{r \neq s}^n M_{r,s}]}{4}} dt \end{aligned}$$

For a fixed  $t$ , we note that  $F^{d_i+1}(t)(1 - F^{d_i+1}(t))$  is a random function as it depends on the degree of the sampled respondents. By taking expectation, we have the following expression,

$$\mathbb{E} [\sum_{i=1}^n F^{d_i+1}(t)(1 - F^{d_i+1}(t))] = \frac{1}{\binom{|P|}{n}} \sum_{i=1}^{|P|} \sum_{\bar{d}_i=0}^{d_i} \binom{d_i}{\bar{d}_i} \binom{|P|-d_i-1}{n-\bar{d}_i-1} F^{\bar{d}_i+1}(t)(1 - F^{\bar{d}_i+1}(t))$$

where  $d_i$  is the degree of respondent  $i$  in the population<sup>2</sup>. Taking reference to Assumption 1, we assume that  $\mathbb{E} [\sum_{r \neq s}^n M_{r,s}] = O(\langle d \rangle^2 n)$ , where  $\langle d \rangle$  is the average degree of the initial population graph and remain in the same order after the sampling process. For the second row in the upper bound, we similarly have

$$\begin{aligned} & \mathbb{E} \left[ \sigma \sqrt{2(1 - \rho^{F, \tilde{F}})} + \sigma + \frac{\sigma}{n} \sum_{i=1}^n \frac{\sqrt{2(1 - \rho^{F^{d_i+1}, \tilde{F}^{d_i+1}}) - 1}}{\sqrt{d_i+1}} \right] \\ & = \sigma \sqrt{2(1 - \rho^{F, \tilde{F}})} + \sigma + \frac{\sigma}{n \binom{|P|}{n}} \sum_{i=1}^{|P|} \sum_{\bar{d}_i=0}^{d_i} \binom{d_i}{\bar{d}_i} \binom{|P|-d_i-1}{n-\bar{d}_i-1} \frac{\sqrt{2(1 - \rho^{F^{\bar{d}_i+1}, \tilde{F}^{\bar{d}_i+1}}) - 1}}{\sqrt{\bar{d}_i+1}} \end{aligned}$$

Combining both terms and splitting the square-root term, we have the following bound,

$$\begin{aligned} \mathbb{E} [W_1(\hat{F}_n, F)] & \leq \frac{1}{n} \int_{\mathbb{R}} \sqrt{\frac{1}{\binom{|P|}{n}} \sum_{i=1}^{|P|} \sum_{\bar{d}_i=0}^{d_i} \binom{d_i}{\bar{d}_i} \binom{|P|-d_i-1}{n-\bar{d}_i-1} F^{\bar{d}_i+1}(t)(1 - F^{\bar{d}_i+1}(t))} dt \\ & \quad + \sigma \sqrt{2(1 - \rho^{F, \tilde{F}})} + \sigma + \frac{\sigma}{n \binom{|P|}{n}} \sum_{i=1}^{|P|} \sum_{\bar{d}_i=0}^{d_i} \binom{d_i}{\bar{d}_i} \binom{|P|-d_i-1}{n-\bar{d}_i-1} \frac{\sqrt{2(1 - \rho^{F^{\bar{d}_i+1}, \tilde{F}^{\bar{d}_i+1}}) - 1}}{\sqrt{\bar{d}_i+1}} \\ & \quad + \frac{O(\langle d \rangle)}{\sqrt{n}} \end{aligned}$$

## Appendix C Statistical results

Distribution	Interaction Rule	Independent	Random	Cluster
Beta(2,2)	Average	0.012	0.016	0.016
	Weighted	0.012	0.016	0.016
Beta(2,5)	Average	0.009	0.012	0.012
	Weighted	0.009	0.012	0.012
Normal(0,1)	Average	0.057	0.084	0.084
	Weighted	0.057	0.084	0.084

Table 2: Mean 1-Wasserstein distance for E-R graphs with edge probability  $4 \times 10^{-6}$

<sup>2</sup>We follow the convention that if  $k < 0$  then  $\binom{n}{k} = 0$

Distribution	Interaction Rule	Independent	Random	Cluster
Beta(2,2)	Average	0.012	0.016	0.016
	Weighted	0.012	0.016	0.016
Beta(2,5)	Average	0.009	0.012	0.012
	Weighted	0.009	0.012	0.012
Normal(0,1)	Average	0.058	0.085	0.085
	Weighted	0.058	0.085	0.085

Table 3: Mean 1-Wasserstein distance for E-R graphs with edge probability  $8.9 \times 10^{-5}$

Distribution	Interaction Rule	Independent	Random	Cluster
Beta(2,2)	Average	0.014	0.030	0.038
	Weighted	0.014	0.025	0.038
Beta(2,5)	Average	0.011	0.021	0.032
	Weighted	0.011	0.018	0.027
Normal(0,1)	Average	0.069	0.130	0.195
	Weighted	0.069	0.115	0.165

Table 4: Mean 1-Wasserstein distance for E-R graphs with edge probability 0.002

Distribution	Interaction Rule	Independent	Random	Cluster
Beta(2,2)	Average	0.032	0.137	0.141
	Weighted	0.032	0.128	0.132
Beta(2,5)	Average	0.023	0.094	0.097
	Weighted	0.022	0.088	0.091
Normal(0,1)	Average	0.153	0.571	0.584
	Weighted	0.153	0.536	0.552

Table 5: Mean 1-Wasserstein distance for E-R graphs with edge probability 0.048

Distribution	Interaction Rule	Independent	Random	Cluster
Beta(2,2)	Average	0.056	0.166	0.168
	Weighted	0.057	0.162	0.160
Beta(2,5)	Average	0.043	0.115	0.116
	Weighted	0.043	0.112	0.110
Normal(0,1)	Average	0.273	0.703	0.696
	Weighted	0.274	0.685	0.675

Table 6: Mean 1-Wasserstein distance for E-R graphs with edge probability 0.211

Distribution	Interaction Rule	Independent	Random	Cluster
Beta(2,2)	Average	0.084	0.176	0.177
	Weighted	0.084	0.172	0.169
Beta(2,5)	Average	0.062	0.122	0.123
	Weighted	0.062	0.119	0.117
Normal(0,1)	Average	0.394	0.746	0.736
	Weighted	0.394	0.731	0.715

Table 7: Mean 1-Wasserstein distance for E-R graphs with edge probability 0.460

Probability	Strategies	Statistic
$4 \times 10^{-6}$	Independent	0.001
	Random	0.012
	Cluster	0.014
$8.9 \times 10^{-5}$	Independent	0.010
	Random	0.034
	Cluster	0.028
0.002	Independent	0.030
	Random	0.258*
	Cluster	0.402*
0.048	Independent	0.028
	Random	0.770*
	Cluster	0.648*
0.211	Independent	0.038
	Random	0.836*
	Cluster	0.824*
0.460	Independent	0.032
	Random	0.928*
	Cluster	0.986*

Table 8: Kolmogorov-D statistic from 2-sample K-S test for E-R graph, average v.s. weighted interaction rule under Beta(2,2) distribution,  $p$ -value  $< 0.01$  (\*)

Probability	Strategies	Statistic
$4 \times 10^{-6}$	Independent	0.002
	Random	0.008
	Cluster	0.012
$8.9 \times 10^{-5}$	Independent	0.010
	Random	0.030
	Cluster	0.040
0.002	Independent	0.032
	Random	0.202*
	Cluster	0.392*
0.048	Independent	0.024
	Random	0.728*
	Cluster	0.626*
0.211	Independent	0.040
	Random	0.724*
	Cluster	0.760*
0.460	Independent	0.024
	Random	0.770*
	Cluster	0.906*

Table 9: Kolmogorov-D statistic from 2-sample K-S test for E-R graph, average v.s. weighted interaction rule under Beta(2,5) distribution,  $p$ -value  $< 0.01$  (\*)



Probability	Strategies	Statistic
$4 \times 10^{-6}$	Independent	0.002
	Random	0.008
	Cluster	0.016
$8.9 \times 10^{-5}$	Independent	0.008
	Random	0.026
	Cluster	0.016
0.002	Independent	0.028
	Random	0.188*
	Cluster	0.33*
0.048	Independent	0.022
	Random	0.700*
	Cluster	0.488*
0.211	Independent	0.040
	Random	0.724*
	Cluster	0.76*
0.460	Independent	0.024
	Random	0.770*
	Cluster	0.906*

Table 10: Kolmogorov-D statistic from 2-sample K-S test for E-R graph, average v.s. weighted interaction rule under standard normal distribution,  $p$ -value  $< 0.01$  (\*)

Distribution	Interaction Rule	Independent	Random	Cluster	Independent (10)	Independent (30)
Beta(2,2)	Average	0.018	0.131	0.132	0.082	0.048
	Weighted	0.018	0.114	0.125	0.082	0.048
Beta(2,5)	Average	0.013	0.090	0.091	0.061	0.035
	Weighted	0.013	0.078	0.086	0.061	0.035
Normal(0,1)	Average	0.095	0.473	0.524	0.385	0.230
	Weighted	0.094	0.477	0.526	0.385	0.230

Table 11: Mean 1-Wasserstein distance for directed EU-email dataset

Distribution	Interaction Rule	Independent	Random	Cluster	Independent (10)	Independent (30)
Beta(2,2)	Average	0.014	0.117	0.127	0.082	0.048
	Weighted	0.014	0.110	0.122	0.082	0.048
Beta(2,5)	Average	0.011	0.081	0.088	0.061	0.035
	Weighted	0.011	0.076	0.084	0.061	0.035
Normal(0,1)	Average	0.070	0.462	0.512	0.385	0.230
	Weighted	0.070	0.461	0.511	0.385	0.230

Table 12: Mean 1-Wasserstein distance for undirected EU-email dataset

Distribution	Interaction Rule	Independent	Random	Cluster	Independent (10)	Independent (30)
Beta(2,2)	Average	0.312*	0.217*	0.284*	0	0
	Weighted	0.312*	0.290*	0.232*	0	0
Beta(2,5)	Average	0.260*	0.906*	0.230*	0	0
	Weighted	0.276*	0.284*	0.212*	0	0
Normal(0,1)	Average	0.352*	0.218*	0.258*	0	0
	Weighted	0.350*	0.292*	0.220*	0	0

Table 13: Kolmogorov-D statistic from 2-sample K-S test for directed against undirected EU-email dataset,  $p$ -value  $< 0.01$  (\*)